University of Nebraska - Lincoln

DigitalCommons@University of Nebraska - Lincoln

Fall 12-5-2019

Optimal Allocation of Energy Storage and Wind Generation in Power Distribution Systems

Carlos Mendoza
University of Nebraska - Lincoln, carlos.mendoza-santos@huskers.unl.edu

Follow this and additional works at: https://digitalcommons.unl.edu/elecengtheses

Part of the Other Electrical and Computer Engineering Commons, and the Power and Energy Commons

OPTIMAL ALLOCATION OF ENERGY STORAGE AND WIND GENERATION

IN POWER DISTRIBUTION SYSTEMS

by

Carlos Alberto Mendoza Santos

A THESIS

Presented to the Faculty of

The Graduate College at the University of Nebraska

In Partial Fulfilment of Requirements

For the Degree of Master of Science

Major: Electrical Engineering

Under the Supervision of Fred Choobineh

Lincoln, Nebraska

December, 2019

OPTIMAL ALLOCATION OF ENERGY STORAGE AND WIND GENERATION

IN POWER DISTRIBUTION SYSTEMS

Carlos Alberto Mendoza Santos, M.S.

University of Nebraska, 2019

Adviser: Fred Choobineh

The advent of energy storage technologies applications for the electric power system gives new tools for planners to cope with the operation challenges that come from the integration of renewable generation in medium voltage networks. This work proposes and implements an optimization model for Battery Energy Storage System (BESS) and distributed generation allocation in radial distribution networks. The formulation aims to assist distribution system operators in the task of making decisions on energy storage investment, BESSs' operation, and distributed generation penetration's level to minimize electricity costs. The BESSs are required to participate in energy arbitrage and voltage control. In addition, due to the complexity of the model formulated, a genetic algorithm combined with an AC multi-period optimal power flow implementation is used to solve the problem. The methodology provides the optimal connection points and size of a predetermined number of BESSs and wind generators, and the BESS's operation. The model considers the BESSs' charging/discharging efficiency, depth of discharge level, and the network's operation constraints on the nodal voltage and branches power flow limits. The proposed methodology was evaluated in the IEEE 33-bus system. The results show that BESSs investment in radial distribution systems facilitates the deployment of distributed generation and favors the reduction of generation costs despite its still high capital cost.

DEDICATION

To Elvira and Cruz

ACKNOWLEDGMENTS

I would like to thank my advisor, Dr. Fred Choobineh, from the Electrical and Computer Engineering Department at the University of Nebraska-Lincoln (UNL) for all his guidance and patience through the course of this research. I also would like to thank Jairo Cervantes for his comments and advice regarding the modeling part of this work.

My sincere gratitude to my thesis committee members, Dr. Jerry Hudgins and Dr. Sohrab Asgarpoor, for their valuable suggestions and insights.

I would like to thank the Fulbright Program and the Electrical and Computer Engineering Department at UNL for sponsoring my masters degree.

I also appreciate Lisbeth Vallecilla for her support in the revision of this thesis and all her guidance during my years of graduate school at UNL.

Finally, I want to thank my family for all their love, support, and understanding of my time away from them.

TABLE OF CONTENTS

LIST OF FIGURES

LIST OF TABLES

CHAPTER 1. OVERVIEW

1.1 Motivation

The increasing penetration of renewable Distributed Generation (DG) is a common trend around the world. This trend is the result of the global environmental concerns, the introduction of competition in electric power markets, and the need for diversification of energy sources as a mechanism to ensure sustainability [10].

According to statistics of the International Renewable Energy Agency (IRENA), the global-installed electric power of renewable energy generation from wind, sun, biomass, and geothermal has been annually growing between 8% and 9%. Furthermore, in recent years, its growth rate is above the rate of non-renewable traditional sources of power generation. Additionally, wind and solar are the renewable sources that are growing faster worldwide (see figure 1.1).

Similarly, in its Short-Term Energy Outlook report, January 2019, the the U.S. Energy Information Administration agency estimated that "The electric generation at utility level of solar projects will grow 10% by 2019 and around 17% in 2020. Likewise, wind generation will grow by 12%-14% in the coming two years" [11].

One of the reasons that justify the increase of generation projects in distribution networks are the attractive installation costs for investments in medium voltage networks. The installation costs are very dependent on the voltage level of the network [12].

This trend is highly disrupting the planning and operation of today's distribution systems because their design have traditionally been conceived as a
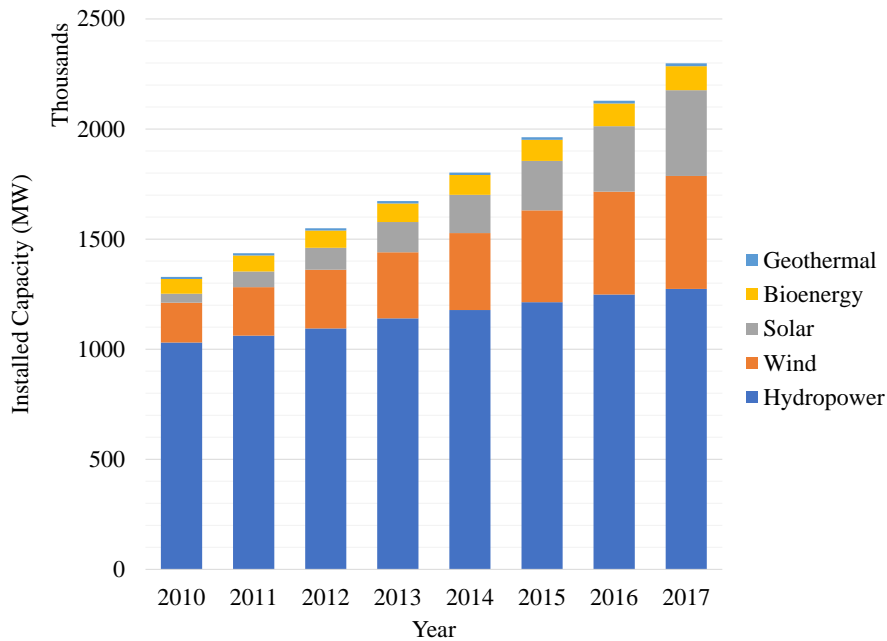
Figure 1.1. Global renewable energy power installed capacity. Adapted from [1].

passive network with unidirectional power flows. These conditions, combined with the uncertainty from the power output of most common utility-scale generation, wind and solar, make distribution systems technically and economically vulnerable to DG's deployment.

In order to identify the possible impacts of power injections in voltage's profile, system reliability, and losses, distribution system companies (DISCOs) usually carry out load flow studies under probable scenarios of demand and contingencies before making decisions about where to connect embedded generation [12].

When there is no technical feasibility for the DGs installation in the distribution network, the DISCOs usually analyze a) the economic implications of carrying out reinforcements in the network, b) the installation of voltage compensators, and c) operating agreements with the DGs owners on power outputs curtailment in demand-generation's scenarios that may jeopardize the security of the network.

With the advent of energy storage technologies, DISCOs have a new

opportunity to analyze DGs connection impacts on the network's operation. Under the reinforcement plans for DGs placement, DISCOs can consider the installation of storage devices on their feeders to maximize the expected benefit of the embedded generation on the system. In addition, the DISCOs investment in energy storage for medium voltage network can be compensated with benefits, such as energy arbitrage, improvement on network's reliability, voltage's profiles, and reduction of congestion.

1.2 Description of the problem

The growing concern for power systems' ecological footprint has increased the needs to diversify the energy resources through the installation of environmentally friendly DGs. These needs can come into conflict with the efficient operation of today's electric power systems if the DGs' incorporation is not optimally planned. Moreover, the penetration of DGs can have greater impacts on distribution networks where the condition of radiality predominates. Some of these conflicts can be mitigated with the addition of storage system in the network.

Despite a large body of research in the distributed energy storage area, studies that considers the addition of both DGs and Battery Energy Storage Systems (BESSs) units while participating in reactive power management in the network were not found. Therefore, this study proposes an optimization model to allocate both BESSs and DGs in the form of wind generation while considering the BESSs' reactive power management capabilities. The proposed model will identify the optimal size and connection point of a predetermined number of wind generators and BESSs in a set of feasible nodes of a distribution network to minimize the utility's electricity cost. For the proposed methodology, the BESSs will participate in the task of voltage control and energy arbitrage.

1.3   Objectives

1.3.1   General objective

The general objective of this work is to develop an optimization model to determine the connection buses and capacity for DG-Wind generators and size-location for BESSs to minimize the cost of supplying the electricity demand in a distribution network.

1.3.2   Specific objectives

1. Identify a model that allows the estimation of wind power penetration's impacts on radial medium voltage network's operation in steady state condition.

2. Identify BESS models for optimization problems considering battery efficiency, state of charge, and active-reactive power operation.

3. Identify the different benefits on radial distribution systems for BESSs and Wind generation allocation.

4. Define strategies for the daily operation of the BESSs base on electricity prices, wind speed, and system load demand's predictions.

1.4   Contributions

The main contribution of this study is to present an optimization model that will support the DISCOs' decision-making process of BESS and DG-wind generations allocation to maximize their expected benefits through electricity cost's reduction.

CHAPTER 2. LITERATURE REVIEW

2.1   Distributed generation in distribution systems

Distributed generation (DG) is usually addressed as power units with capacity smaller than 10 MW and in proximities to the final consumers in distribution grids [13]. Its rate of penetration in the power system is growing faster in the recent years due to governmental policies, decreasing costs of technology , and the global environmental awareness. The new scenario aims to reduce the emission of greenhouse gases through the promotion of renewable sources, and the efficient use of energy [14].

The DGs connection networks have traditionally been designed to meet the energy demand radially. Furthermore, the voltage control has been carried out through load-tap-changing transformers at the main node of the system, voltage regulator transformers, shunt capacitor banks, and reactors located on the main feeders [13].

Although the incorporation of generation facilities close to the end users in distribution grids can enhance the efficiency and reliability of the electric power service provision, the increase in the deployment of not optimally allocated DG in utility networks can introduce significant alterations in its operation, and disrupt its voltage regulation [15].

In addition, high penetration of DG may lead to modification of the power flows in such a way that an increase in the system energy losses may occur. All these conditions combined with the intermittency of most DGs, based on wind and

solar energy, and the stochastic nature of the electric power demand hinder its integration in distribution networks.

A detailed study of the effects of distributed generation on radial utility network is presented in [13]. The research exposes the scenarios on which the connection of embedded generation must be considered to avoid affecting the operation of the electric system. The paper analyzes the impact on the networks voltage regulation, losses, power quality, and short circuit levels. Likewise, reference [16] investigates additional technical implications of DGs power injections on overcurrent protection, insulation, and instantaneous feeder reclosers.

Different strategies have been proposed to solve the problem of siting and sizing DG in distribution networks to reduce their impact on this type of systems. The study in [17] presents a summary of the objectives that are commonly pursued by utilities in this context. According to this research, optimization models have been developed with different objectives. For instance, a) minimizing the network losses, b) maximizing the system reliability, c) maximizing cost-benefit ratio for the DISCOs, and d) minimizing network voltage fluctuation. In addition, due to the complexity of solving the optimization problems (nonlinear-noncovex), and the size of the systems, optimization methods such as: non linear programming, dynamic programming, and heuristic methods such as: genetic algorithm, particle swarm optimization, and differential evolution, have been used.

A technical approach for increasing the penetration of wind generation in radial distribution systems is proposed in [12]. In this study, operations actions were analyzed to identify their support on the network security, and reliability improvement. Generation curtailment, reactive power compensators deployment, and On-Load Tap changer (OLTC) area-based voltage control were investigated as methods to overcome the impacts of power injections. It was found that with these methods, and mainly with the area-based voltage control coordination through

OLTCs, the network's hosting capacity of distributed generation is effectively improved.

2.2   Battery Storage System (BESS) in distribution networks

To cope with the operation challenges and facilitate the incorporation of DG in distribution networks, new technologies are expected to be deployed in distribution systems [18]. One of these new technologies is the Battery Energy Storage System (BESS). The BESSs are made up of an energy storage devices such as batteries, and a power conversion system (PCS) designed with voltage source inverters to operate as an inverter (DC/AC) and as a rectifier (AC/DC) [19].

Additionally, the incorporation of BESS to the network can provide advantages to both, the distribution network operators, and DG owners. Some of these advantages are: a) reduction of electricity tariff through energy arbitrage, b) deferral of investment in network expansion, c) increase in the penetration of DG due to the minimization of power curtailment, and d) improvement in the system reliability [17]. Despite all these benefits, due to the still high cost of BESS, an optimal siting, sizing, and operation, is required for a cost-effective deployment.

Because of the promising support of BESSs to power systems, and the expected decrease of their capital cost in the futures years, the problem of their integration into distribution networks have been subject of research of several authors in the academia. The researches have been looking to reduce the negative impacts of DGs, and make their deployment attractive to Distribution System Companies (DISCOs), and DG owners.

Considering the challenges that unpredictable power generation poses to the planning and operation of medium voltage systems, most of the studies have focused on optimization methodologies to increase the flexibility of the electric network to host DG [20]- [21]. Among the studies, BESSs have been widely used to buffer the

intermittence of most DGs, to reduce their impact on voltage regulation, and to decrease the power imported from the main grid in peak hours demand (Peak Shaving).

In [20] a methodology is presented to locate and size ESS in distribution networks in the context of a high penetration of wind energy. The objective of this study is to minimize the curtailment on wind generation balancing the benefits to both DISCOs and DG owners. In order to place and size ESS units, the research uses the prediction of hourly wind energy production and electric demand along a year combined with prices of electricity for DG power. The annual benefits of the deployment of Distributed Energy Storage Systems (DESS) for the DISCOs and wind generator owners is compared with the investment required for several ESS technologies. This model disregards the reactive power injection capacity of the ESSs units.

The study in [22] presents an optimal power flow model considering both active and reactive power generated by distributed wind power units and BESSs. The proposed methodology takes advantages of the BESSs' PCS to minimize the energy losses and support the voltage regulation of distribution networks. The model uses the demand, and wind generation profiles to establish the optimal power dispatch, curtailment of the DG, and charging/discharging conditions of the BESSs in the system. The BESSs are considered with the capacity of injecting reactive power while being discharged and absorb it in their process of charging. This research was analyzed over a two-tariff price model, on-peak, and off-peak demand tariff. The results show that optimizing both reactive and active power in a distribution network with generation and storage capacity can substantially reduce the energy losses and the reactive power imported from the main grid.

In [23] is proposed a strategy to incorporate distributed energy storage systems (DESS) in the context of smart grids (SG) to maximize the benefits for the medium

and high voltage networks. The method optimally allocates DESSs and capacitor banks minimizing the network losses, the reactive power provided by the main grid and DGs units, the electricity cost, the investment in DESS and capacitor banks, and the network's reinforcement needs over a specified planning period. This work also explores the benefits that DESS can generate in smart grid systems considering energy price arbitrage in different regulatory frameworks and applications. The optimization model is solved using genetic algorithm and sequential quadratic programming. The first stage used a genetic algorithm to locate and size the DESSs and the capacitor banks. In the second stage, the sequential quadratic programming method was adopted to determine the optimal operating conditions of the DESSs daily rate of charge/discharge, and the reactive power injected by the DESSs and DGs units to the system. In this study, the maximum reactive power provided by the DESS is restricted to its power rating.

A methodology is proposed in [24] to size and place BESS in distribution system with embedded solar generation. In this study, the BESS is used to alleviate voltage variations due to intermittent current injections from solar energy plants. For this task is presented a formulation based on the matrix impedance of the system to operate, size and locate the BESS considering its inverters active and reactive power capabilities.

The research in [21] presents a methodology to optimally size, locate, and operate BESSs units to maximize the benefits to DISCOs under the scenario of high-power injections from photovoltaic generation units. The objective function of the proposed model considers the investment and maintenance cost of BESSs and its participation on energy arbitrage, environmental emission, energy losses, and transmission fees reduction. Additionally, this study does not exploit the BESSs ability to provide reactive power support to the network. The optimization model was solved using a genetic algorithm and the linear programming technique.

Few studies of BESSs integrating to distribution system considering the stochasticity of power demand, generation, and electricity cost were found. Jacob et al. in [25] present an optimization problem for BESS sizing using the point estimation method to model the randomness of these variables. The particles swarm optimization algorithm was used to solve the formulated model.

A research for optimal allocation of DGs and BESSs in distribution networks is presented in [26]. In this study, a deterministic optimization model is proposed for reducing energy losses, reverse power, and voltage fluctuations through the deployment and operation of BESSs and DGs. The optimization problem locates and sizes a set of BESSs and wind turbines using a genetic algorithm. In that study the PCS' BESSs reactive power capacity was not considered.

CHAPTER 3. BATTERY ENERGY STORAGE TECHNOLOGIES

An electric battery is a system that stores energy in a chemical medium for a period of time to be discharged in electricity's form in the future. The first electrochemical cells battery was developed by Alessandro Volta in the eighteenth century. It was called voltaic pile and consisted of a circuit of two different metal electrodes separated by an electrolyte. This configuration was able to generate an electric current using chemical reactions [27].

A battery consists of a set of cells arranged in series, parallel, or both to reach an objective voltage , and a nominal power-energy capacity at their terminals. The BESS is used to refer to the set of storage modules; a) local protections, b) battery energy systems, c) racking frames at DC level, d) the balance of system (BOS). The BOS is composed of monitors/control, containers, HVAC/thermal management, communication, and fire suppression equipment [28]. These components form the energy storage module, power conversion system (PCS), and the power plant controller. For practical applications, the BESS instantaneous power capacity, and maximum energy output are determined by the storage module and the power conversion systems rating. The instantaneous power is defined as the maximum capacity of the inverter for a given operating condition in MW, or kW. In addition, the maximum energy output is established by the energy storage module and corresponds to its storage capacity in MWh, or kWh [29]. The capital cost of a BESS usually consist of the storage module, the balance of system, engineering procurement, and construction [30]. Among the parameters that are commonly

taken into account when choosing a battery technology are the efficiency, life span, operating temperature, depth of discharge, self-discharge rate, and energy density [31].

There is a large range of commercialized battery energy storage technologies. Below some of the technologies most widely used at utility scale are described.

3.1 Lithium-ion (Li-ion) batteries

Lithium-ion batteries are considered a well-developed energy storage technology that has been traditionally used in electronic devices. In recent years, due to the advancement in the electric transportation industry, their prices are constantly falling. This condition has made them attractive to applications in the electric power system area. A Li-Ion battery is rechargeable storage device that commonly consists of a negative electrode (anode) made of a carbon porous material, a positive electrode (cathode) made of a metal oxide, and Lithium salt as electrolyte [32]. A current flow of Lithium ions travels from the cathode to the anode (see figure 3.1) in the process of the battery charging, and in the opposite direction in the discharging stage. The principal advantages of this technology are its high energy density, low self-discharge, large charging efficiency, and the potential development of applications to allow faster charging and discharging rates. Their expected life cycle in current implementations is between 5 to 10 years [29].
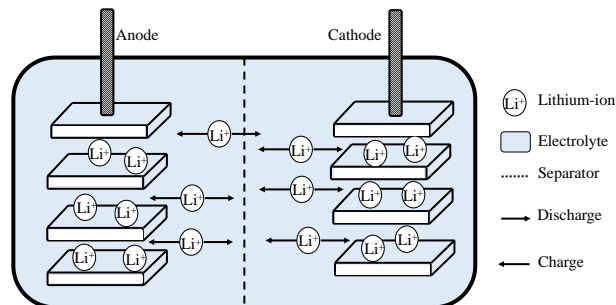
Figure 3.1. Lithium-ion Battery. Adapted from [2].

3.2 Flow batteries

A Flow battery is an energy storage technology that stores energy in liquid electrolytes. The battery consists of two electrolytes made from a solution of metallic salts such as vanadium and zinc-bromine that flow in different chambers separated by a membrane (see figure 3.2). An electric current is generated by the induction of a reduction-oxidation reaction that allows ions exchange through the membrane. Its nominal energy and power capacity are determined by the volume of the electrolytes and the electrolytes surface, respectively. The storage of electrolytes in different containers reduces the risks of their implementation to the point that this technology is generally considered to be safer than traditional batteries. This condition makes flow batteries attractive for applications at the electric power systems level [33]. Flow batteries are known for their long cycle life, sizing flexibility (their nominal power and energy capacity can be adjusted separately according to the volume of the electrolytes and the area of the ions exchange membrane). Since the chemical reactions during the process of charging and discharging occur in the liquid electrolytes, they can reach a low state of charge without significant effect on their cycle life. Their expected life service is between 10 and 20 years [29]. Additionally, their low round-trip efficiency and energy density are considered among their disadvantages.
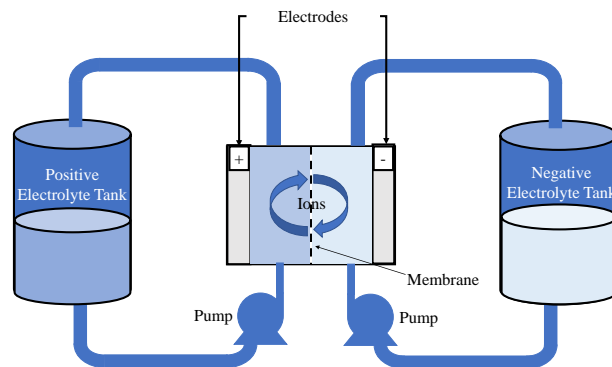
Figure 3.2. Flow battery energy storage technology. Adapted from [3].

3.3   Lead-acid batteries

Lead-acid batteries are one of the oldest electrochemical energy storage technology. They have been used in a considerable number of applications such as cars, planes, off-grid systems, and uninterruptible power supplies [30]. Additionally, in the power system, Lead batteries are commonly used as back up energy source in substation and generation plants [34]. There are two types of Lead-acid batteries, flooded and valve regulated. Flooded batteries, also known as vented lead-acid battery, are made of a lead Pb negative electrode and lead-dioxide , PbO_2, positive electrode submerged in an electrolyte of a solution of sulfuric acid H_2SO_4. A Flooded Lead-acid battery is depicted in figure 3.3. In the discharging process, chemical reactions transform the electrodes into $PbSO_4$, and the solution of sulfuric acid progressively turns to be mostly water. In the charging process, the electrolytes are returned to lead dioxide and lead. Valve regulated lead acid batteries uses a overpressure valve that operates for pressure levels above 100 millibars inside the battery. The valve principally reduces the maintenance cost of the battery through the reduction of the electrolyte solution's water loss [4]. The efficiency of batteries under this technology is between 80 and 90%. In addition, their capacity decreases deeply when high power is discharged from them [35].
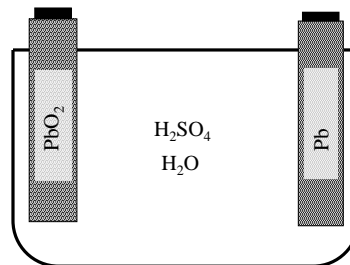
Figure 3.3. Lead-acid battery. Adapted from [4].

3.4 Sodium sulfur (NaS) batteries

Sodium-sulfur batteries are an energy storage technology that uses as electrodes molten salts of sulfur in the cathode and sodium in the anode. The electrodes are separated by a solid sodium-alumina electrolyte that only allows the flow of positive sodiums ions, see figure 3.4. During the discharging process, 2 volts are generated in the battery's terminals through a current of sodium ions in the electrolyte that turns into electrons in the external circuit. The charging process reverses the chemical reactions, the sodium ions are generated back to neutralize the sodium electrode [36].
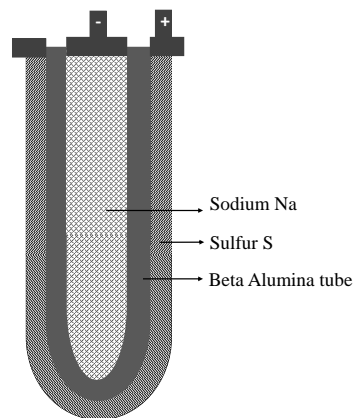
Figure 3.4. Sodium sulfur (NaS) battery. Adapted from [5].

This type of battery is characterized by a long-life service, their expected cycle of life is 10 years, and a high charging/discharging efficiency [28]. Because their operating temperature is higher than 300 degrees Celsius, they are mostly designed for commercial and utility scale stationary projects. The first utility scale sodium sulfur battery was a storage system of 1 MW and 8 MWh designed with 26880 cells by 1990s. Manufacturers produce battery units base on modules of 10 to 50kW and 50 to 400 kWh. They arrange the modules in series-parallel to reach the objective voltage, power, and energy [37].

CHAPTER 4. BESS AND WIND GENERATOR ALLOCATION MODEL

This chapter describes an optimization model for BESS, and Wind generation allocation in the distribution network. The formulation considers the operator of the distribution system as the investor in BESS. Additionally, the DISCO will not build or operate the wind generators. This will be carried out by an external investor. The model provides the installation bus and size of a set of BESS units and Wind generators while considering as restrictions the system operation limits and batteries constraints. The notation used in this chapter is detailed in appendix A.

4.1 Optimization model proposed

The objective of this optimization model is to minimize the cost of supplying the system demand through the deployment of BESSs and wind generation in the network. The proposed model considers a predefined maximum number of BESSs and wind power generators to install in a set of feasible buses. For the analysis, the model's decision variables are the installation bus and size of the BESSs and wind generators. Additionally, a set of representative periods of 24 hours of power demand, wind speed, and electricity cost are considered by the model to estimate the DISCOs expected benefits. In this model it is assumed that the wind generators will be required to operate at a power factor equal to one.

Equation 4.1 presents the objective function of the optimization problem. The first term of the equation corresponds to the BESS' capital cost per day. In this formulation, a battery base unit is used to determine the BESS' total capital cost.

C^B is the battery base unit's cost per day. The factor φ_i^B is an integer variable used to identify the number of battery units to install in a bus i in the set of feasible buses Ω^{N_f}. This variable indicates the size of each BESS to place in the system. The battery base unit is defined by its maximum energy capacity in kWh and nominal power rating in kVA. x_i^B is a binary variable that indicates the installation of a BESS in a bus i. This variable is used to limit the number of buses with battery energy storage systems.

The second term of the equation defines the expected daily cost of supplying the system's electricity demand. C_t^E represents the hourly electricity cost, $p_{i=1,t}^{Grid}$ is the power imported from the grid at time t. $(\varphi_i^{DG} \cdot P_t^W)$ represents the power output of the generators installed at bus i at time t. To determine the size of the wind generator to place in the system, a predefined wind turbine will be used as a base unit for the model. i.e. the optimization problem will identify the number of base unit wind turbines to install in a bus i in Ω^{N_f}. In this equation, φ_i^{DG} is the number of wind turbines in the power plant, and P_t^W is the power output of the base wind turbine unit according to the expected wind speed in the geographical area under study. Ω^T corresponds to the set of periods of analysis and Δt is the duration of each period in hours.

$$\min_\Delta z = \sum_{i \in \Omega^{N_f}} C^B \cdot x_i^B \cdot \varphi_i^B + \sum_{t \in \Omega^T} \left[C_t^E \cdot p_{i=1,t}^{Grid} + \sum_{i \in \Omega^{N_f}} C_t^E \cdot \varphi_i^{DG} \cdot P_t^W \right] \cdot \Delta t \quad (4.1)$$

The problem's constraints are presented by equation 4.2 through equation 4.30. Equation 4.2 corresponds to the nodal real power balance at the reference bus over all periods of analysis. Likewise, equation 4.3 determines the nodal reactive power balance at the same bus.

$$P_{i,t}^D + p_{i,t}^{ch,B} - p_{i,t}^{dis,B} + P_{i,t} - p_{i,t}^{Grid} - \varphi_i^{DG} \cdot P_t^W = 0, \quad i = 1, \ \forall t \in \Omega^T \qquad (4.2)$$

$$Q_{i,t}^D + q_{i,t}^B + Q_{i,t} - q_{i,t}^{Grid} = 0, \quad i = 1, \ \forall t \in \Omega^T \tag{4.3}$$

Similarly, equation 4.4 and 4.5 corresponds to the nodal real and reactive power balance, respectively, at all the system's buses except the reference node.

$$P_{i,t}^D + p_{i,t}^{ch,B} - p_{i,t}^{dis,B} + P_{i,t} - \varphi_i^{DG} \cdot P_t^W = 0, \quad \forall i \in \Omega^N, i \neq 1, \ \text{and} \quad \forall t \in \Omega^T \tag{4.4}$$

$$Q_{i,t}^D + q_{i,t}^B + Q_{i,t} = 0, \quad \forall i \in \Omega^N, i \neq 1, \ \text{and} \quad \forall t \in \Omega^T \tag{4.5}$$

Equation 4.6 and equation 4.7 represent the real and reactive power output, respectively, from bus i at each period of analysis t through the branches connected to the bus i.

$$P_{i,t} = v_{i,t} \sum_{j \in \Omega^N} v_{j,t} Y_{i,j} \cos\left(\delta_{i,t} - \delta_{j,t} - \theta_{i,j}\right), \quad \forall i \in \Omega^N, \ \text{and} \quad \forall t \in \Omega^T \tag{4.6}$$

$$Q_{i,t} = v_{i,t} \sum_{j \in \Omega^N} v_{j,t} Y_{i,j} \sin\left(\delta_{i,t} - \delta_{j,t} - \theta_{i,j}\right), \quad \forall i \in \Omega^N, \ \text{and} \quad \forall t \in \Omega^T \tag{4.7}$$

Similarly, equation 4.8 and equation 4.9 are used to determine the real and reactive power flow, respectively, from bus i to bus j.

$$P_{i,j,t} = v_{i,t}^2 Y_{i,j} \cos(\theta_{i,j}) - v_{i,t} v_{j,t} Y_{i,j} \cos\left(\delta_{i,t} - \delta_{j,t} - \theta_{i,j}\right), \forall i, j \in \Omega^N, \ \text{and} \quad \forall t \in \Omega^T \tag{4.8}$$

$$Q_{i,j,t} = -v_{i,t}^2 Y_{i,j} \sin(\theta_{i,j}) - v_{i,t} v_{j,t} Y_{i,j} \sin\left(\delta_{i,t} - \delta_{j,t} - \theta_{i,j}\right), \forall i, j \in \Omega^N, \ \text{and} \quad \forall t \in \Omega^T \tag{4.9}$$

The BESS model's equality constraints used in this work are presented from equation 4.10 to equation 4.14. This formulation considers the BESS' state of charge and charging/discharging periods. The stored energy in the BESSs at every period t is determined by equation 4.10. In this formulation, η_{ch}/η_{dis} represent the BESS's charging/discharging efficiency.

$$E_{i,t}^B = E_{i,t-1}^B + \left[\eta_{ch} \cdot p_{i,t}^{ch,B} - \frac{p_{i,t}^{dis,B}}{\eta_{dis}}\right] \Delta t, \quad \forall i \in \Omega^{N_f}, \text{ and } \quad \forall t \in \Omega^T \tag{4.10}$$

Equation 4.11 establishes the BESS' maximum energy storage capacity. $\overline{E}^{B_u}$ is the BESS' base unit maximum energy storage capacity.

$$\overline{E}_i^B = \varphi_i^B \cdot \overline{E}^{B_u}, \quad \forall i \in \Omega^{N_f} \tag{4.11}$$

In addition, equation 4.12 corresponds to the lower bound of the BESS's energy level. This equation takes into account the BESS base unit's depth of discharge, DoD^{B_u}, restriction.

$$\underline{E}_i^B = (1 - DoD^{B_u}) \cdot \overline{E}_i^B, \quad \forall i \in \Omega^{N_f} \tag{4.12}$$

Here it is assumed that the stored energy in every BESS at $t = 0$ and $t = T$ is equal to $\underline{E}_i^B$, which means that all days of analysis will start and end with the same amount of energy in the BESSs. This condition is defined in equation 4.13.

$$E_{i,t=0}^B = E_{i,t=T}^B = \underline{E}_i^B, \quad \forall i \in \Omega^{N_f} \tag{4.13}$$

The BESS's maximum apparent power limit is given by equation 4.14.

$$\overline{S}_i^B = \varphi_i^B \cdot \overline{S}^{B_u}, \quad \forall i \in \Omega^{N_f} \tag{4.14}$$

The equality constraints in equation 4.15 is used to set the reference bus objective angle at all the period of analysis.

$$\delta_{i,t} = 0.0, i = 1 : ref, \quad \forall t \in \Omega^T \tag{4.15}$$

In this model, for a single bus either a wind generator or a BESS will be installed, but not both. The restriction in equation 4.16 is used to satisfy this condition.

$$x_i^{DG} \leq (1 - x_i^{B}) \quad \forall i \in \Omega^{N_f} \tag{4.16}$$

Equation 4.17 defines the branches apparent power constraint.

$$P_{i,j,t}^2 + Q_{i,j,t}^2 \leq \overline{S}_{i,j}^2 \quad \forall i, j \in \Omega^N, i \neq j, \text{ and } \quad \forall t \in \Omega^T \tag{4.17}$$

Similarly, equation 4.18 defines BESS' apparent power constraint.

$$\left(p_{i,t}^{ch,B} - p_{i,t}^{dis,B}\right)^2 + \left(q_{i,t}^{B}\right)^2 \leq \left(\overline{S}_i^{B}\right)^2, \forall i \in \Omega^{N_f}, \text{and} \quad \forall t \in \Omega^T \tag{4.18}$$

In order to determine the size of the BESSs and wind generators only in the buses where x_i^B and x_i^{DG} are equal to one, the constraints in equation 4.19 and equation 4.20 are considered.

$$\varphi_i^B \leq x_i^B M \tag{4.19}$$

$$\varphi_i^{DG} \leq x_i^{DG} M \tag{4.20}$$

Equation 4.21 and equation 4.22 are used to limit the number of BESS and wind generator to install, respectively. N^B corresponds to the maximum number of BESS and N^{DG} the maximum number of wind generators to place in the network.

$$\sum_i x_i^B \leq N^B \quad \forall i \in \Omega^{N_f} \tag{4.21}$$

$$\sum_i x_i^{DG} \leq N^{DG} \quad \forall i \in \Omega^{N_f} \tag{4.22}$$

The system wind power penetration is limited through equation 4.23. In this equation, the total wind generation's installed power is restricted to the main

substation's power capacity. This constraint is used to avoid conditions where the exporting power from the utility network is above the limits of the main substation.

$$\sum_i \varphi_i^{DG} \cdot P^{TBnom} \leq \overline{P}^{Sub} \quad \forall i \in \Omega^{N_f} \tag{4.23}$$

Equation 4.24 defines the upper and lower bound of the BESS' energy storage capacity.

$$\underline{E}_i^B \leq E_{i,t}^B \leq \overline{E}_i^B \quad \forall i \in \Omega^{N_f}, \text{ and } \quad \forall t \in \Omega^T \tag{4.24}$$

Equation 4.25 and equation 4.26 correspond to the nodal voltage magnitude and angle's operating limits, respectively.

$$\underline{V} \leq v_{i,t} \leq \overline{V}, \quad \forall i \in \Omega^N, \text{ and } \quad \forall t \in \Omega^T \tag{4.25}$$

$$-\pi \leq \delta_{i,t} \leq \pi, \quad \forall i \in \Omega^N, \text{ and } \quad \forall t \in \Omega^T \tag{4.26}$$

Equation 4.27 and 4.28 define the upper and lower bound of the BESS' maximum charging, and discharging power, respectively.

$$0 \leq p_{i,t}^{ch,B} \leq \overline{S}_i^B, \quad \forall i \in \Omega^{N_f}, \text{ and } \quad \forall t \in \Omega^T \tag{4.27}$$

$$0 \leq p_{i,t}^{dis,B} \leq \overline{S}_i^B, \quad \forall i \in \Omega^{N_f}, \text{ and } \quad \forall t \in \Omega^T \tag{4.28}$$

The BESS's reactive power limits correspond to equation 4.29.

$$-\overline{S}_i^B \leq q_{i,t}^B \leq \overline{S}_i^B, \quad \forall i \in \Omega^{N_f}, \text{ and } \quad \forall t \in \Omega^T \tag{4.29}$$

Equation 4.30 is the linear approximation of a wind turbine power curve function of the wind speed. Taking into account that most distribution systems are

restricted in a relatively small area with the same geographical conditions, the generator's power output installed in the system will be calculated assuming a uniform wind speed in the whole distribution network in every period of analysis t.

$$P_t^W = \begin{cases} 0 & , \quad v_{wind}(t) < v_{c_{in}} \text{ or } v_{wind}(t) > v_{c_{out}} \\ \left(\frac{v_{wind}(t) - v_{c_{in}}}{v_r - v_{c_{in}}}\right) P^{TB_{nom}} & , \quad v_{c_{in}} \leq v_{wind}(t) \leq v_r \\ P^{TB_{nom}} & , \quad v_r < v_{wind}(t) < v_{c_{out}} \end{cases} \tag{4.30}$$

Finally, the decision variables of the problem are the following:

$$\Delta = \{x_i^B, \varphi_i^B, x_i^{DG}, \varphi_i^{DG}, p_{i,t}^{Grid}, q_{i,t}^{Grid}, v_{i,t}, \delta_{i,t}, p_{i,t}^{ch,B}, p_{i,t}^{dis,B}, q_{i,t}^B\} \quad \forall i \in \Omega^N, \quad \text{and } \forall t \in \Omega^T$$

4.2 Solution approach for the BESS and wind generator allocation problem.

The proposed allocation model is a nonlinear mixed integer problem (MINLP) that is very complex to solve. In this section, an approach to solve the model using the evolutionary optimization method genetic algorithm (GA) is presented. The proposed MINLP can be expressed in the following standard form:

$$\min_{\Delta} f_{inv}(\Delta) + f_{op}(\Delta)$$

Subject to,

$$g(\Delta) = 0 \tag{4.31}$$

$$h(\Delta) \leq 0$$

$$\Delta_{\min} \leq \Delta \leq \Delta_{\max}$$

$$\Delta = \left[x_i^B, \varphi_i^B, x_i^{DG}, \varphi_i^{DG}, p_{i,t}^{Grid}, q_{i,t}^{Grid}, v_{i,t}, \delta_{i,t}, p_{i,t}^{ch,B}, p_{i,t}^{dis,B}, q_{i,t}^B\right], \quad \forall i \in \Omega^N, \quad \text{and } \forall t \in \Omega^T$$

Where, $f_{inv}(\Delta)$ is associated with the BESSs investment and is a function of a

BESS base unit daily capital cost, and $f_{op}(\Delta)$ is the system 24-hours optimal operation. The network's operation subproblem is a well known AC optimal power flow (AC-OPF) where it fully considers the system AC power flow with the incorporation of energy storage's restrictions. In addition, the hourly analysis requirements become the problem in a multi-period AC-OPF. The model's equality constraints consider the nodal active and reactive power balance. The inequality constraints take into account the network branches and BESS PCSs apparent power limits, the nodal voltage and BESSs energy bounds, and charging-discharging power lower and upper limits.

In general, the problem's multi-period condition, its AC-Network formulation, and the substantially high number of options for BESS-Wind generation allocation that may arise depending on the feasible locations set's size, make this problem challenging to solve. GA is a metaheuristic technique for large combinatorial optimization problems commonly used to find solutions to complex models where the traditional optimization methods do not perform well. Additionally, in the power system field, different GA applications have been proposed for problems such as distributed generation allocation, [38], optimal power flow, [39], and unit commitment, [40].

GAs are intelligent searching methods for global optimization inspired by biological evolution. They start with a randomly selected population that evolves toward the optimum through natural selection strategies in an iterative process. GAs encode individual properties in a chromosome string over which the algorithm applies genetic operators. The first operator is called selection and consists of evaluating the individuals based on their fitness value. The individuals with better fitness value have a greater probability of surviving to the next generation. The second operator is known as crossover. In this, the parents' chromosomes, individuals that survived from the previous generation, are combined with a certain

probability to create children. The last operator, mutation, consists of introducing random modifications to some individuals' chromosomes to create new children. The individuals' evolutionary process is carried out repeatedly until a stopping condition is reached. [38], [41].

As was previously stated, the formulated problem can be considered as an optimization problem where there are two subproblems. The first one is the investment and the second is the network operation optimization. In order to find a solution to the problem using GA, the operation subproblem will be solved using MATPOWER, an open-source Matlab set of functions for power system analysis [42]. An AC multi-period optimal power flow (AC-MPOPF) will be implemented and solved using the MATPOWER Interior Point Solver (MIPS).

The MATPOWER's AC-MPOPF implementation will receive as input the system network parameters, the nodal voltage and branches limits, the hourly electricity rates, the BESS location, and size parameters, and the wind generators connection bus and power injection profile according to the wind speed's expected value, and their power rating. The network configuration will be considered fixed in this study, i.e through the GA iterations, the network structure will not change.

The result of the AC-MPOPF will be the hourly real and reactive power imported from the grid, and the BESS operation (charging and discharging period, and the reactive power absorption or injection) that minimizes the cost of supplying the demand. From this, the problem decision variables will be the connection node and size of the BESSs and wind generators to install in the system. The GA algorithm will provide the optimal combination of BESS and wind generators' location and size to minimize the objective function satisfying the wind generators' installed power constraint in equation 4.23. Each feasible individual in the GA's population will encode the decision variables in a chromosome as figure 4.1. The length of the encoded string will depend on the number of BESSs and wind

generators to install in the system. As it can be seen in the figure, each BESS and wind generator requires two positions in the encoded string for its location and size, respectively.
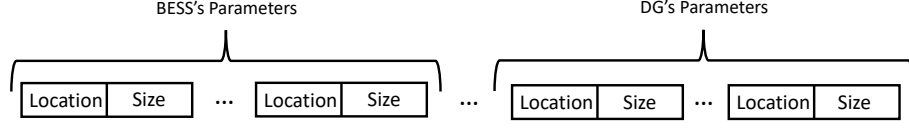
Figure 4.1. GA individuals encoding of a chromosome.

Taking into account that the MATPOWER AC-MOPF will provide the system's optimal operation for every combination of BESS-Wind generation's size and connection bus, the problem's objective function in equation 4.31 will be redefined as follows:

$$\min_{\hat{\boldsymbol{\Delta}}} f_{inv}(\hat{\boldsymbol{\Delta}}) + f_{op}(\hat{\boldsymbol{\Delta}}) + F^{Wind}(\hat{\boldsymbol{\Delta}}) \tag{4.32}$$

In this equation, $F^{Wind}(\hat{\boldsymbol{\Delta}})$ corresponds to a penalty function that represents the inequality constraint for the maximum wind generation installed capacity in the system, see equation 4.33, where ω is a penalty factor. $\hat{\boldsymbol{\Delta}}$ is the GA individuals' chromosome where is encoded the BESSs and wind generators connection bus and size. In this part, the new variables (χ_s^B, Φ_s^B) are used to represent the location and size, respectively, for every BESS in the set of BESSs to install. Similarly, $(\chi_s^{DG}, \Phi_s^{DG})$ determine the connection bus and size, respectively, of every wind generator to install in the system.

$$F^{Wind}(\hat{\boldsymbol{\Delta}}) = \begin{cases} \omega \cdot \left(\sum_{s=1}^{N_{DG}} \Phi_s^{DG} \cdot P^{TB_{nom}} - \overline{P}^{Sub} \right)^2, & \sum_{s=1}^{N_{DG}} \Phi_s^{DG} \cdot P^{TB_{nom}} > \overline{P}^{Sub} \\ 0 & , \quad \text{otherwise} \end{cases} \tag{4.33}$$

$$\hat{\boldsymbol{\Delta}} = \{\boldsymbol{\chi^B}, \boldsymbol{\Phi^B}, \boldsymbol{\chi^{DG}}, \boldsymbol{\Phi^{DG}}\}$$

In this work, the MATLAB's GA implementation available in its global optimization toolbox will be used. The input parameters for the GA's objective function will be the set of feasible buses for BESS-wind generator installation and the feasible number of units to be added. Since a fully AC network formulation will be considered, there may be BESS-wind generation allocation's combinatory options where the MIPS does not converge, in these cases, the GA's individual will be penalized and considered unfeasible, i.e its fitness value will be adjusted to a large number. Figure 4.2 presents a flowchart of the GA approach proposed in this study.
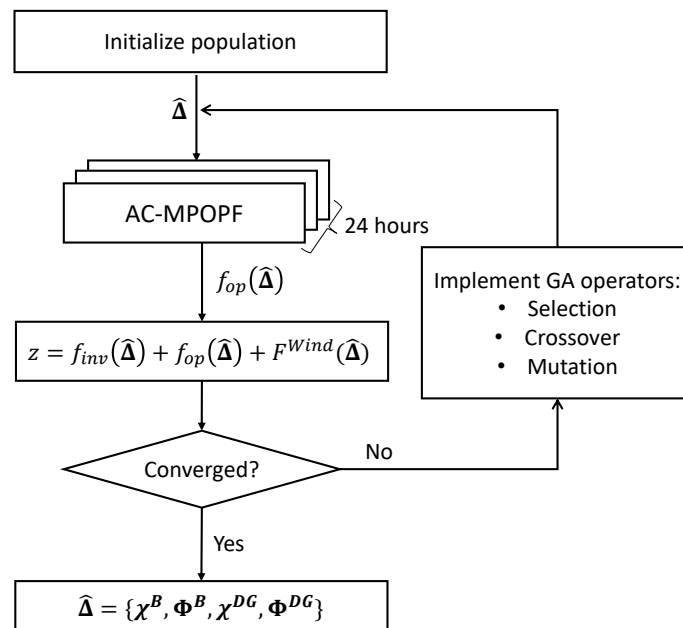
Figure 4.2. GA's Flowchart.

CHAPTER 5. MULTI-PERIOD OPTIMAL POWER FLOW

The model's operation subproblem is an AC-MPOPF where the cost of supplying the demand has to be minimized. An AC-MPOPF allows DISCOs to make decisions about BESSs and network's operation considering the estimated energy prices, electricity demand and the wind generators' power injections in every period of analysis. In this work, the AC-MPOPF will be solved using MATPOWER, which is an open-source set of MATLAB functions for electric power system analysis in steady-state [42]. This application has the advantage that allows the extension of the standard optimal power flow formulation throughout user additional cost function, variables, linear and non-linear constraints.

5.1 MATPOWER Optimal Power Flow

In MATPOWER, the standard formulation of an AC-OPF is expressed as follows:

$$\min_x f(x)$$

$$\text{Subject to,}$$

$$g(x) = 0 \tag{5.1}$$

$$h(x) \leq 0$$

$$x_{\min} \leq x \leq x_{\max}$$

Where, the objective function $f(x)$ represents the cost of supplying the energy

demand and is determined by the generation cost's curve of each generator in the system. The equality constraints of the problem, $g(x) = 0$, corresponds to the nodal power balance. The loading levels in elements such as transmission lines and transformers are restricted through $h(x) \leq 0$. Similarly, the vectors of nodal voltage magnitudes V_m, angles δ and generators power outputs, P_g, Q_g, are constrained by $x_{min} \leq x \leq x_{max}$. In this formulation, the optimization variable is defined by $x = (\delta, V_m, P_g, Q_g)$, which is a vector of length equal to $2 * N_B + 2 * N_g$, where N_B is the system's number of buses and N_g is the number of generators.

In addition, in its extended form, the MATPOWER AC-OPF corresponds to the previous model with the user customized variables, objective function, and constraints. The general formulation of this case is the following:

$$\min_{\hat{x}} f(x) + f_u(\hat{x})$$

$$\text{Subject to,}$$

$$\hat{g}(\hat{x}) = 0$$

$$\hat{h}(\hat{x}) \leq 0 \tag{5.2}$$

$$\hat{x}_{min} \leq \hat{x} \leq \hat{x}_{max}$$

$$l \leq A\hat{x} \leq u$$

In equation 5.2, the variable $\hat{x} = (x, z)$ is an extension of x, from the formal AC-OPF problem, with the user's new variable z and objective function, $f_u(\hat{x})$. The bounds for the problem's decision variables, including z, are defined through $\hat{x}_{min} \leq \hat{x} \leq \hat{x}_{max}$. The matrix A, vectors l and u are used to implement user linear inequality constraints. A is the constraints' coefficients matrix of size $n \times m$, where n is the number of linear inequality constraints, and m is the number of decision variables, i.e., the length of $\hat{x}$. l and u are, respectively, the lower and upper bound limits of the linear inequality constraints.

5.2   MATPOWER AC-MPOPF Implementation

Since there is not a direct way to perform an AC-MPOPF in MATPOWER, its optimal power flow function will be adapted to the problem formulated in figure 4.1 using its AC-OPF structure and code customization capabilities. When there is not a BESS in the system, the the optimal operation subproblem studied in this work can be solved running T times a standard AC-OPF. However, this condition changes when a BESS is added to the problem. As it can be noticed in equation 4.10, the BESS' state of charge in an instant t is linked to its previous state. Due to these requirements, the AC-MPOPF problem will be implemented in the following steps.

1. The system network will be replicated T times to represent all the cases in Ω_T, where T is the number of periods of analysis, see figure 5.1, i.e. the final network in MATPOWER will have T islanded networks each one representing the state of the system in every period. In addition, in each of these sub-networks the system demand, wind generator power output and electricity cost will be adjusted according to their expected value.

2. The BESSs will be modelled as two generators that represent the BESS's charging, and discharging periods. These generators will have real and reactive power restrictions equal to their operation limits, see equations 4.18 , 4.27, 4.28, and 4.29.

3. Equation 4.10 will be added to the MATPOWER AC-OPF function as a linear inequality constraint with the limits presented in 4.24. In addition, as required by equation 5.2, a matrix of coefficients, A, based on the BESSs connection nodes will be created. As it can be noticed from 4.10 the energy in a BESS is a linear function of the power charged ($p_{i,t}^{ch,B}$) or discharged ($p_{i,t}^{dis,B}$) from the battery at every period.

4. The upper and lower bounds of equation 4.24 will be added to the MATPOWER's model as the vector l and u in equation 5.2.

5. The BESSs nonlinear restriction, equation 4.18, will be implemented in the MATPOWER's AC-OPF formulation as an stantard Matlab function. Details about how to add nonlinear constraints in MATPOWER are presented in [42], section 7.1.
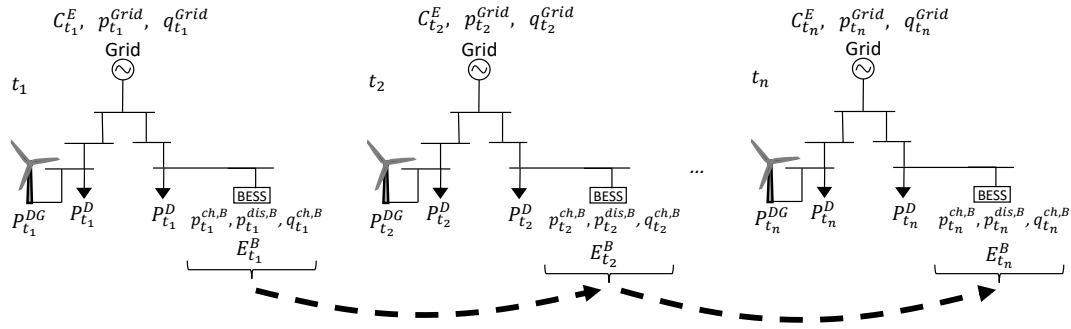
Figure 5.1. MATPOWER AC-MPOPF implementation.

Figure 5.2 shows an example of the implementation of the first step on a small network. As it can be seen, there are two active elements in this network, the main grid (the generator connected to bus 1), and the BESS connected to bus 3. In addition, for this example, in order to analyze the network in a horizon of three periods, $T = 3$, the system has been replicated T times as shown in figure 5.2. With these adjustments, the new network for the multi-period study has nine generators, and nine buses. In figure 5.2, $\{P_1, Q_1\}$, $\{P_2, Q_2\}$, and $\{P_3, Q_3\}$ correspond to the grid's real and reactive power injections in the period, t_1, t_2, and t_3, respectively. Likewise, $\{P_4, Q_4\}$, $\{P_6, Q_6\}$, $\{P_8, Q_8\}$, refer to the BESS's real power absorbed and the reactive power absorbed/injected in the periods, t_1, t_2, and t_3, respectively. $\{P_5\}$, $\{Q_7\}$, $\{P_9\}$ are used to represent the BESS's power injection to the system in the period, t_1, t_2, and t_3, respectively. In MATPOWER, the power absorbed by a

generator is considered negative and positive when the power is injected to the system.

The next procedure has to be followed in order to add to the MATPOWER's AC-OPF model the linear inequality constraint represented by equation 4.10 and equation 4.24. Considering the new buses' numeration shown in figure 5.2, the power charged or discharged from the BESS in every period is defined by the power absorbed/injected at bus 3, 6, and 9. It is important to recall the order of the vectors stored in the MATPOWER's decision variable, $x = (\delta, V_m, P_g, Q_g)$. As a result of this order, some positions of the matrix A have to be equal to zero to configure the linear inequality constraint in equation 4.24. The BESS' stored energy equation is then redefined in equation 5.3. Similarly, the redefined lower l and upper u bounds vectors of the BESS's energy constraint are configured in equation 5.4.
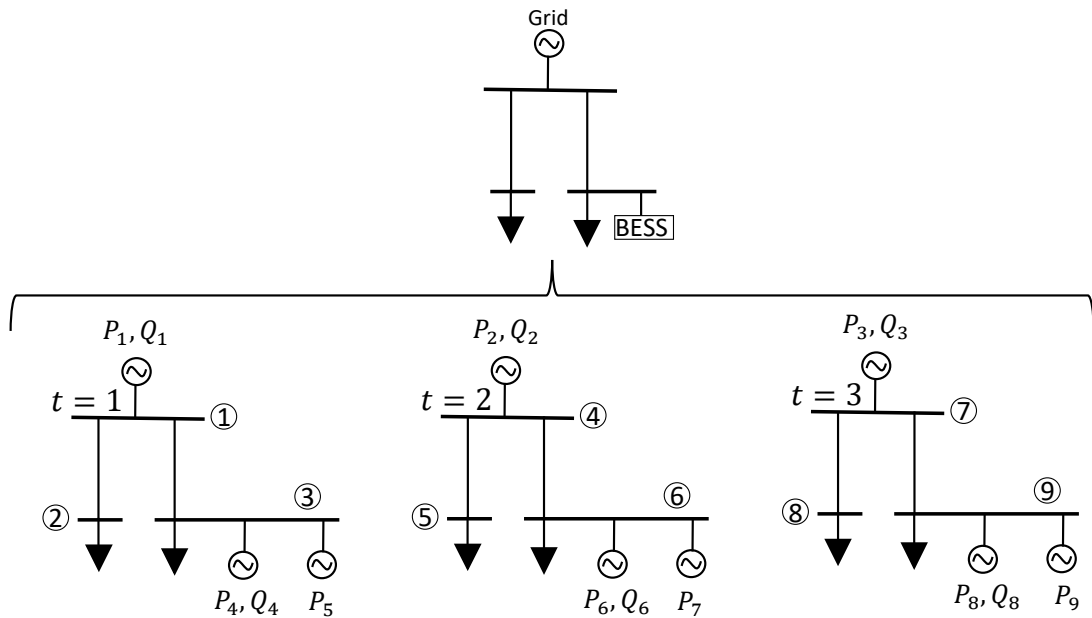
Figure 5.2. MATPOWER AC-MPOPF implementation example.

$$
\begin{bmatrix} E_{t=1}^B \\ E_{t=2}^B \\ E_{t=3}^B \end{bmatrix} - \begin{bmatrix} E_{t=0}^B \\ E_{t=0}^B \\ E_{t=0}^B \end{bmatrix} = \underbrace{\begin{bmatrix} [0]_{1x9} & [0]_{1x9} & [0]_{1x3} & -\eta_{ch} & -\frac{1}{\eta_{dis}} & 0 & 0 & 0 & 0 & [0]_{1x9} \\ [0]_{1x9} & [0]_{1x9} & [0]_{1x3} & -\eta_{ch} & -\frac{1}{\eta_{dis}} & -\eta_{ch} & -\frac{1}{\eta_{dis}} & 0 & 0 & [0]_{1x9} \\ [0]_{1x9} & [0]_{1x9} & [0]_{1x3} & -\eta_{ch} & -\frac{1}{\eta_{dis}} & -\eta_{ch} & -\frac{1}{\eta_{dis}} & -\eta_{ch} & -\frac{1}{\eta_{dis}} & [0]_{1x9} \end{bmatrix}}_{A} \cdot \underbrace{\begin{bmatrix} [\boldsymbol{\delta}]_{9x1} \\ [\boldsymbol{Vm}]_{9x1} \\ [\boldsymbol{P}]_{3x1} \\ P_4 \\ P_5 \\ P_6 \\ P_7 \\ P_8 \\ P_9 \\ [\boldsymbol{Q}]_{9x1} \end{bmatrix}}_{x} \qquad (5.3)
$$

$$
l = \begin{bmatrix} 0 \\ 0 \\ 0 \end{bmatrix}, \; u = (\overline{E}^B - \underline{E}^B) \cdot \begin{bmatrix} 1 \\ 1 \\ 1 \end{bmatrix} \qquad (5.4)
$$

Equation 5.5 corresponds to the BESS' charging power limits. This equation is adjusted to the MATPOWER's OPF model as a regular generator bound.

$$-\overline{S}^B \leq P_4 \leq 0$$
$$-\overline{S}^B \leq P_6 \leq 0 \qquad (5.5)$$
$$-\overline{S}^B \leq P_8 \leq 0$$

Similarly, equation 5.6 is used to represent the BESS' discharging power bounds.

$$0 \leq P_5 \leq \overline{S}^B$$
$$0 \leq P_7 \leq \overline{S}^B \qquad (5.6)$$
$$0 \leq P_9 \leq \overline{S}^B$$

Equation 5.7 corresponds to the BESS's reactive power limits.

$$-\overline{S}^B \leq Q_4 \leq \overline{S}^B$$
$$-\overline{S}^B \leq Q_6 \leq \overline{S}^B \qquad (5.7)$$
$$-\overline{S}^B \leq Q_8 \leq \overline{S}^B$$

Because in this work the MATPOWER Interior Point Solver, MIPS, is going to be used to solve the AC-MPOPF, the BESS's nonlinear inequality constraint, equation 4.18, has to be transformed to equation 5.8.

$$\underbrace{\begin{aligned}(P_4 + P_5)^2 + (Q_4)^2 - \left(\overline{S}^B\right)^2 \leq 0 \\ (P_6 + P_7)^2 + (Q_6)^2 - \left(\overline{S}^B\right)^2 \leq 0 \\ (P_8 + P_9)^2 + (Q_8)^2 - \left(\overline{S}^B\right)^2 \leq 0\end{aligned}}_{h(\boldsymbol{P}, \boldsymbol{Q})} \qquad (5.8)$$

In addition, the solver MIPS requires for the nonlinear inequality constraints a Matlab functions to evaluate the constraints' gradient, $\nabla h\left(\boldsymbol{P}, \boldsymbol{Q}\right)$, and the Hessian

of the constraints term in the Lagrangian function, $\mu^\top h\left(\boldsymbol{P}, \boldsymbol{Q}\right)$, where μ is the Lagrange multiplier of the inequality constraint, i.e $\nabla^2 h\left(\boldsymbol{P}, \boldsymbol{Q}\right)$. Details about the Matlab function implementation of nonlinear inequality constraints for the MIPS can be found in [42], Appendix A.

CHAPTER 6. APPLICATIONS AND RESULTS

In order to demonstrate the validity of the model proposed in this study, a series of simulations were performed on the IEEE 33-Bus test system, see figure 6.1. This configuration consists of a 12.66 kV radial distribution network with maximum real and reactive power load equal to 3715.0 kW and 2300.0 kVar, respectively [8]. The system's parameters are reported in Appendix C.
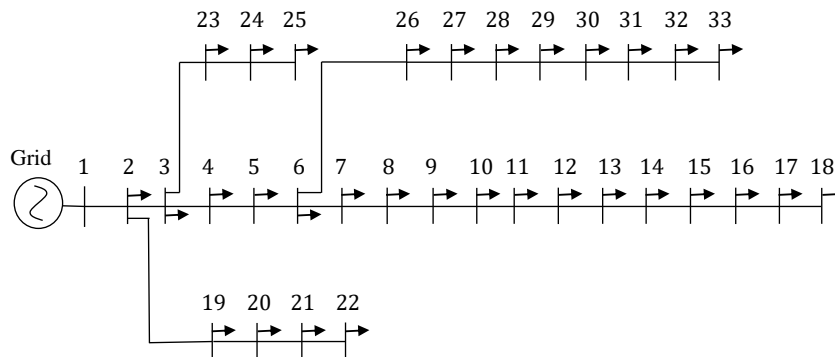
Figure 6.1. IEEE 33-bus radial system.

Figure 6.2 depicts the system's electricity price and demand profiles used in this study. The per-unit value of the power demand and electricity cost correspond to the hourly expected value in a real distribution system. This information was retrieved from historical data of the local marginal price (LMP) and power load in the last five years in Lincoln, NE [43], [6]. The electricity price's curve was adjusted assuming a mean value equal to the U.S. average retail price for residential sectors in March 2018, 12.99 ($cents/kWh$) [44]. In addition, the energy consumption was scaled to the IEEE 33-Bus test system's total demand.
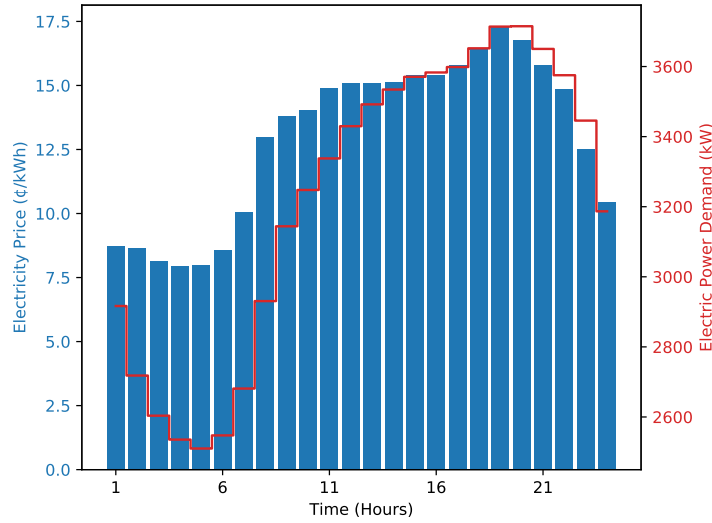
Figure 6.2. Hourly electricity price and power demand.

The load profile, in per unit, shown in figure 6.3, was used to scale the system demand in each period of analysis.
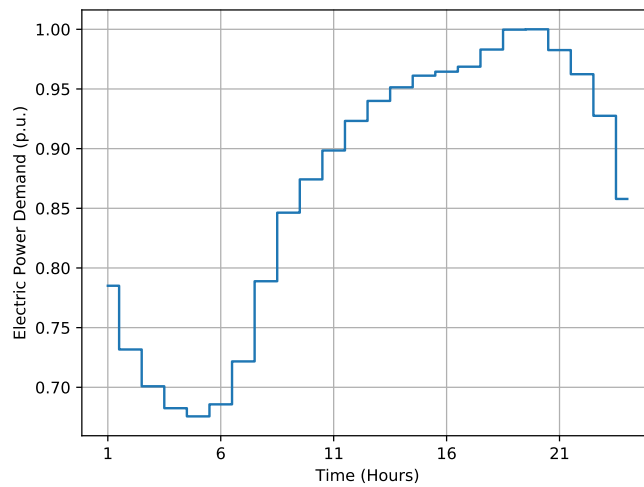
Figure 6.3. System's hourly electricity demand [6].

Similarly, the wind speed's profile in figure 6.4 corresponds to the hourly average of the last five-year in Lincoln, NE, at 10 meters. The wind turbine and BESS's parameters considered in this study are detailed in Appendix C.
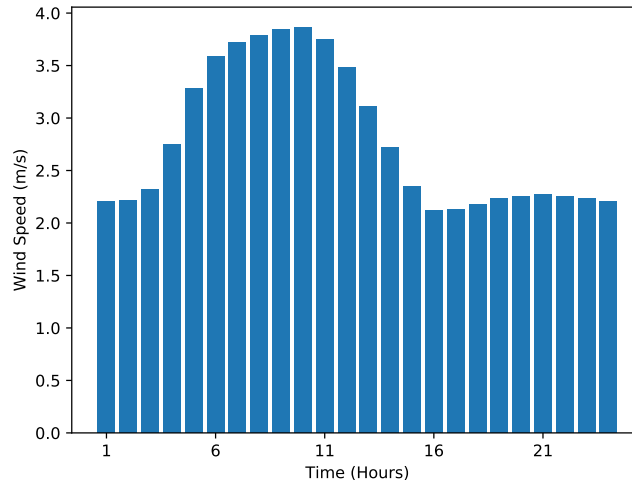
Figure 6.4. Hourly wind speed [7].

6.1 Simulation case 1, the base-case

The base-case simulation is the execution of an AC-MPOPF for 24 hours to identify the initial generation cost and the system's losses without considering the allocation of BESSs and wind generators. From the simulation, the daily electricity cost is equal to $10,795.78$, the total energy demand is 77.3 MWh, and the total energy losses are 3.28 MWh. The system's voltage profile (heat-map) is shown in figure 6.5. As expected, in high demand periods, the tail end buses $29 - 33$, and buses $13 - 18$ at the hours $19 - 21$, had the lowest voltage in $p.u.$. The minimum voltage was found at the bus 18 at the period 19 with a value of 0.9679 $p.u.$.

6.2 Simulation case 2, base-case with DG

The second simulation performed was the optimal siting and sizing of two wind generator without considering the installation of BESSs in the system. For this case, the model's parameters are presented in table 6.1, where ω corresponds to the GA's inequality constraint penalization parameter, see equation 4.33. The possible connection points' options for the wind generators, χ^{DG}, are the bus numbers in the interval $[2, 33]$. Similarly, their size options, Φ^{DG}, are the integer numbers in the
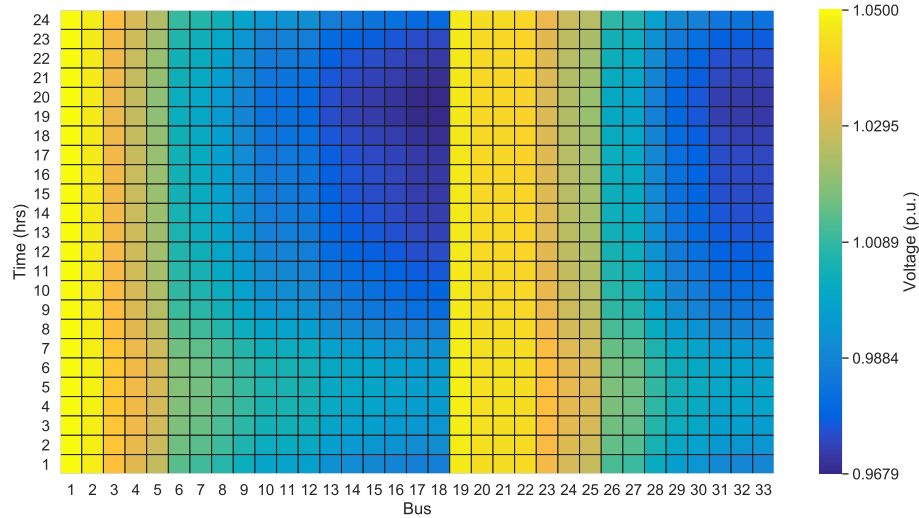
Figure 6.5. System's voltage profiles, initial conditions.

range [0,30]. In order to reduce the number of combinations to considered by the GA, a wind turbine of 198 kW was defined as the base unit, i.e., 33 units of the wind turbine presented in table C.3. According to this, the maximum power of each wind generator to install in the system is equal to $198 * 30$ or 5.94 MW. The main substation power rating capacity $P^{TB_{nom}}$ was assumed to be equal to 6 MVA.

Table 6.1. Simulation's parameters, Case 2.

Parameter	Value
ω	1e6
N^B	0
N^{DG}	2
Ω^{N_f}	{2,...,33}
χ^{DG}	[2,33]
Φ^{DG}	[0,30]
$P^{TB_{nom}}$	6 MVA

The simulation's results show that after optimally allocating two wind generators in the system, the daily electricity cost is equal to $10,663.42$. For a total energy demand of 77.3 MWh and system losses of 2.29 MWh. The connection point and size of the generators are presented in table 6.2. In figure 6.6 is depicted the system voltage profile. As expected, the embedded generation increases the voltage in the buses near to their connection points at the periods of maximum

Table 6.2. Wind generators' allocation, Case 2.

Element	Location	Size
Generator 1	Bus 13	1.386 MW (7 units · 0.198 MW)
Generator 2	Bus 30	1.782 MW (9 units · 0.198 MW)

power injection, $8 - 11$ hrs.
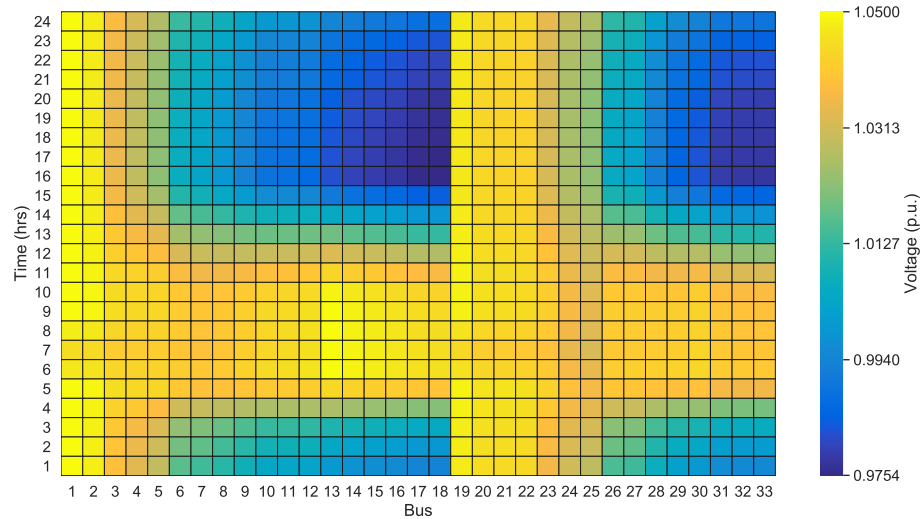
Figure 6.6. System's voltage profiles, Case 2.

Figure 6.7 shows the system's demand profile, and the grid and generators' real power injection. The hours in the range $8 - 11$ hrs are the periods of the maximum real power injection. Similarly, the minimum level of real power imported from the grid is reached in the interval of $6 - 7$ hrs.

6.3 Simulation case 3, base-case with DG and BESS

In order to identify the system's benefits for the optimal allocation of both wind generators and BESSs, the proposed model was solved using the parameters in table 6.3. For this simulation case, a maximum of two wind generators and BESSs were considered for possible addition. The BESS base units' size options to install in the network corresponds to the integer numbers in Φ^B, i.e., the minimum number of BESSs units was configured equal to zero and the maximum equal to 32.
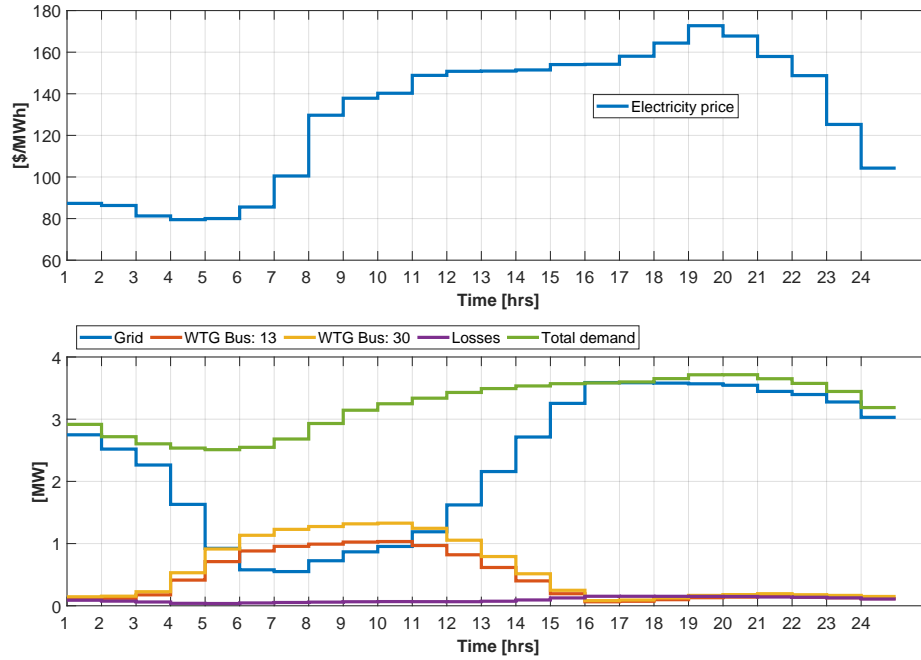
Figure 6.7. System's demand profile and power injection, Case 2.

Table 6.3. Simulation's parameters, Case 3.

Parameter	Value
ω	1e6
N^B	2
N^{DG}	2
Ω^{N_f}	{2,...,33}
χ^{DG}, χ^B	[2,33]
Φ^{DG}	[0,30]
Φ^B	[0,32]
$P^{TB_{nom}}$	6 MVA

The optimal allocation results are presented in table 6.4. The system's generation cost for this case is equal to \$10, 447.51. For a BESS' investment of \$161.80 per day and total losses equal to 1.39 MWh.

The network's voltage profile is shown in figure 6.8. There is a noticeable improvement in the voltage levels for this case. 0.9887 p.u., at the bus 18, in the period 16, was the minimum voltage reached in the system. Similarly, 1.05 p.u., at the bus 1, in the period 17, was the maximum voltage achieved.

Table 6.4. Wind generators and BESS' allocation, Case 3.

Element	Location	Size
Generator 1	Bus 13	1.386 MW (7 units $\cdot$ 0.198 MW)
Generator 2	Bus 29	1.98 MW (10 units $\cdot$ 0.198 MW)
BESS 1	Bus 14	4 units (0.4 MWh, 0.2 MVA)
BESS 2	Bus 30	12 units (1.2 MWh, 0.6 MVA)

The evolution of the network's demand and generation levels, during the 24 hours of analysis, are presented in figure 6.9. From this simulation case, the periods between 3-6 hrs and 18-20 hrs are the moments in the day when the BESSs participate in energy arbitrage. As expected, in the first interval, periods of the lowest electricity prices and demand, the BESSs are charged. Likewise, the BESSs are discharged at the times of the highest electricity rates and demand, i.e., 18-20 hrs.
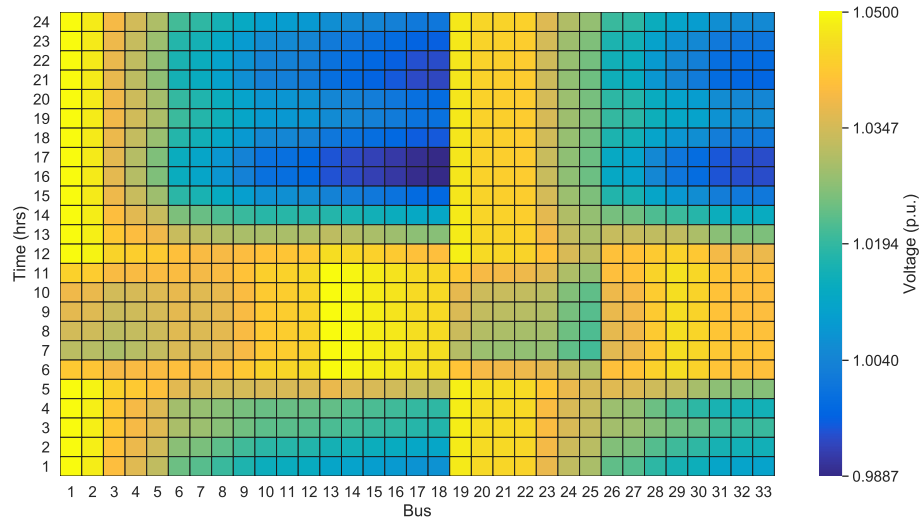
Figure 6.8. System's voltage profiles, Case 3.

Figure 6.10 presents the optimal BESSs' operation in the 24 periods of analysis. This figure shows the participation of the BESSs in the voltage support's task. In the periods in which the BESSs do not store or provide real power to the system, they provide reactive power at the PCS's rated capacity. This condition contributes to the reduction of the system's losses. Figure 6.11 shows the evolution of the energy stored in the BESSs through the time of analysis. As stated in the
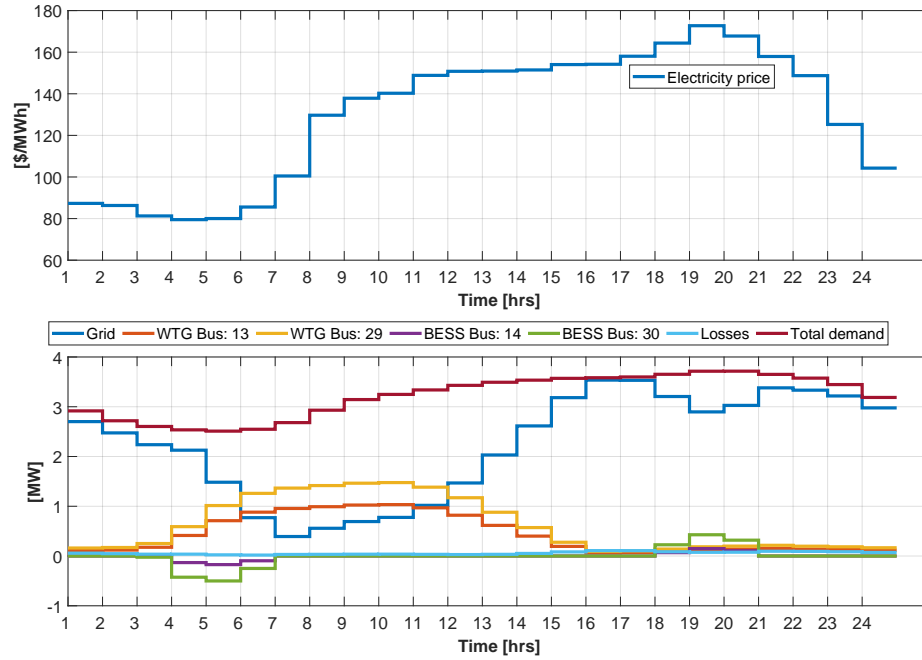
Figure 6.9. System's demand profile and power injection, Case 3.

optimization model, the BESSs are assumed to be partially charged at $t = 0$, see equation 4.13. The BESSs are fully charged at period 6 and remain in this condition until period 17. After period 19, the BESSs stay at its depth of discharge level.

6.4 Simulation case 4, variation in N^{DG} and N^B

In this case, to determine the maximum number of wind generators and BESSs to deploy in the system, a sensitivity analysis was performed for variations of the model's parameters, N^{DG} and N^B. Figure 6.12 shows the system's daily benefits with respect to N^{DG}, and N^B. The results obtained show that when the installation of wind generation in the network is not considered, two or more BESSs have to be allocated in the system to generate a reduction in the system's cost. For $N^{DG} > 0$, increasing N^B produces relatively small increments in the system's benefits. In addition, the reduction of the system's costs stabilizes around \$200 per day as the
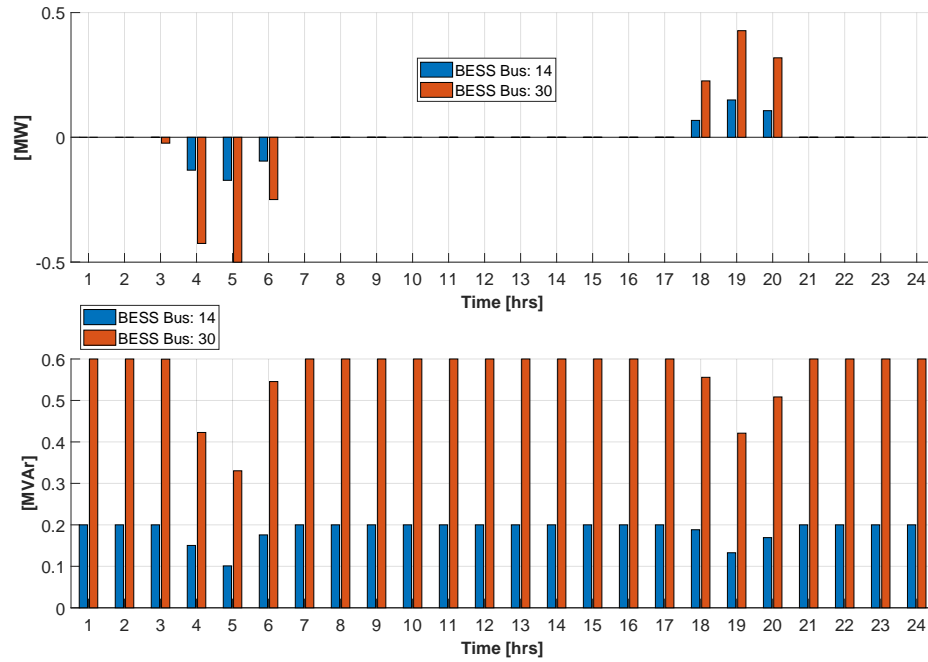
Figure 6.10. BESSs' operation, 24 hrs, Case 3.
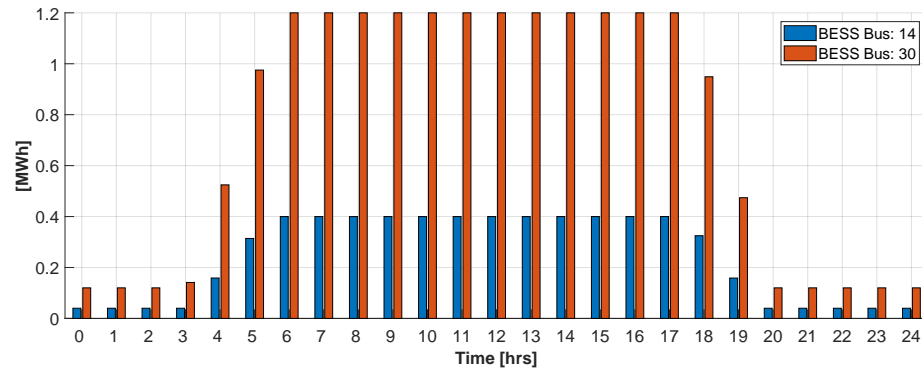
Figure 6.11. Daily energy stored in the BESSs, Case 3.

maximum number of wind generators approaches to five. \$210.17 per day at $N^{DG} = 5$ and $N^B \geq 3$ was the maximum benefit achieved.

Taking into account that in terms of operation, for a DISCO, it is favorable to have the lowest possible number of BESSs in the system, from the sensitivity analysis' outcomes were selected the optimal parameters $N^{DG} = 5$ and $N^B = 3$. The results obtained with this parametrization, for the wind generators and BESSs

connection points and size, are presented in table 6.5. The installed power of wind generation is equal to 5.346 MW. This value is 58.82% greater than the previous case. Considering a higher number of wind generators increases the benefits due to reductions in energy losses. The total losses, installing three BESSs and five wind generators in the system, are equal to 1.22 MWh, a value 12% less than the simulation case 3. The system's generation cost is equal to $10,423.80 per day. For this simulation case, the total energy storage capacity installed in the system remains the same as the previous simulation scenario, however, the energy storage capacity is deployed on a greater number of buses.
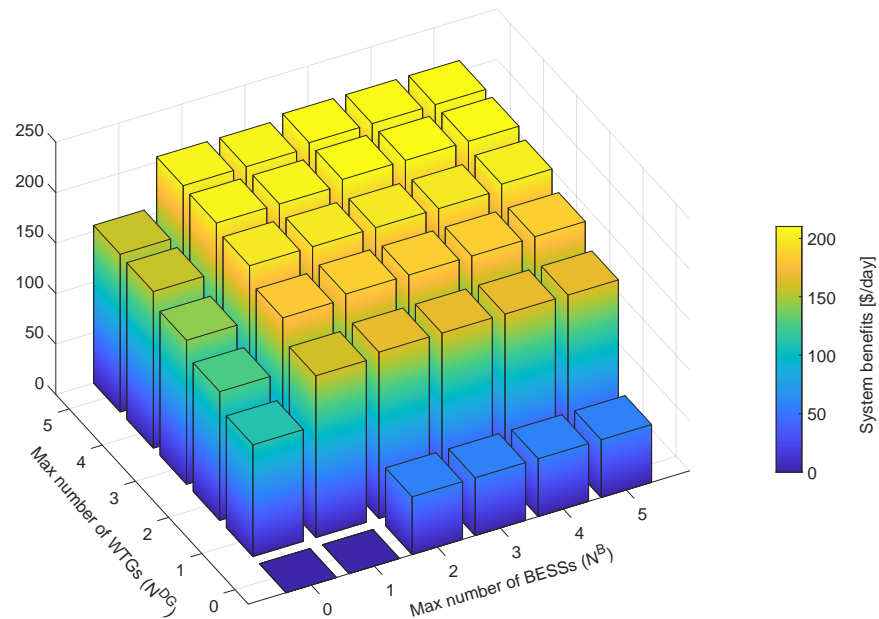
Figure 6.12. System's benefits for variations on N^{DG} and N^B.

The power injection and demand profiles are shown in figure 6.13. In the interval t= 6-11, the distribution system exports power to the grid. Similarly, in figure 6.14 the network's voltage profile is depicted. The minimum voltage in the system is equal to 0.9894 p.u. at the bus 18, in the period 16.

Figure 6.15 presents the optimal BESSs' operation in the 24 periods of analysis.

Table 6.5. Wind generators and BESS' allocation

Element	Location	Size
Generator 1	Bus 3	0.792 MW (4 units $\cdot$ 0.198 MW)
Generator 2	Bus 7	1.188 MW (6 units $\cdot$ 0.198 MW)
Generator 3	Bus 14	0.99 MW (5 units $\cdot$ 0.198 MW)
Generator 4	Bus 25	1.188 MW (6 units $\cdot$ 0.198 MW)
Generator 5	Bus 31	1.188 MW (6 units $\cdot$ 0.198 MW)
BESS 1	Bus 15	4 units (0.4 MWh, 0.2 MVA)
BESS 2	Bus 30	6 units (0.6 MWh, 0.3 MVA)
BESS 3	Bus 32	6 units (0.6 MWh, 0.3 MVA)

Similarly to simulation case 3, the BESSs provide voltage support to the system. In the periods in which the BESSs do not store or supply real power to the network, they provide reactive power at the PCS's rated capacity. This condition contributes to the reduction of the system losses. The evolution of the energy storage in the BESSs is presented in figure 6.16. The BESSs are fully charged at period 6 and remain in this condition until period 17. After period 19, the BESSs stay at its depth of discharge level.
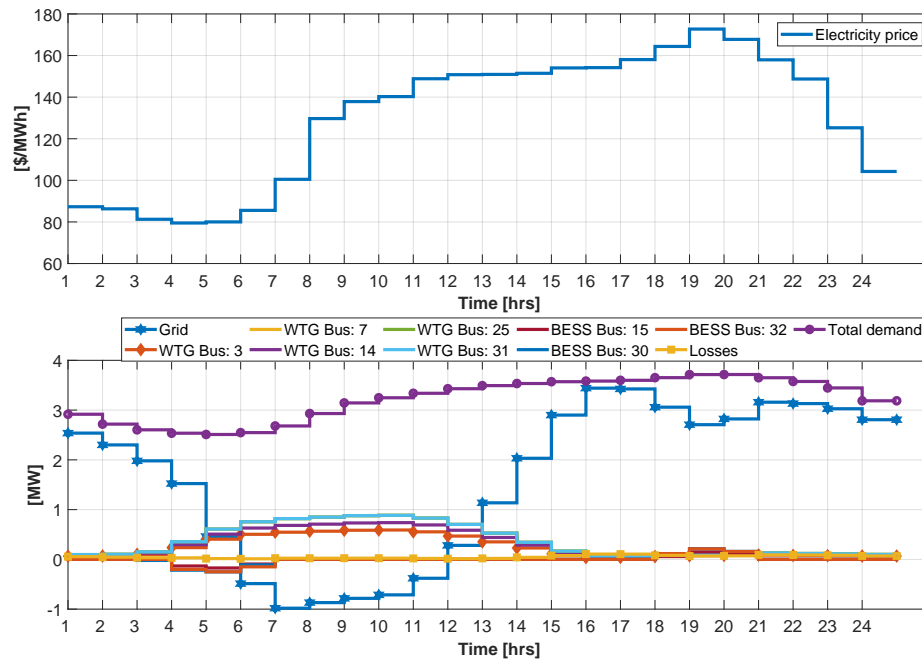
Figure 6.13. System's demand profile and power injection, Case 4.
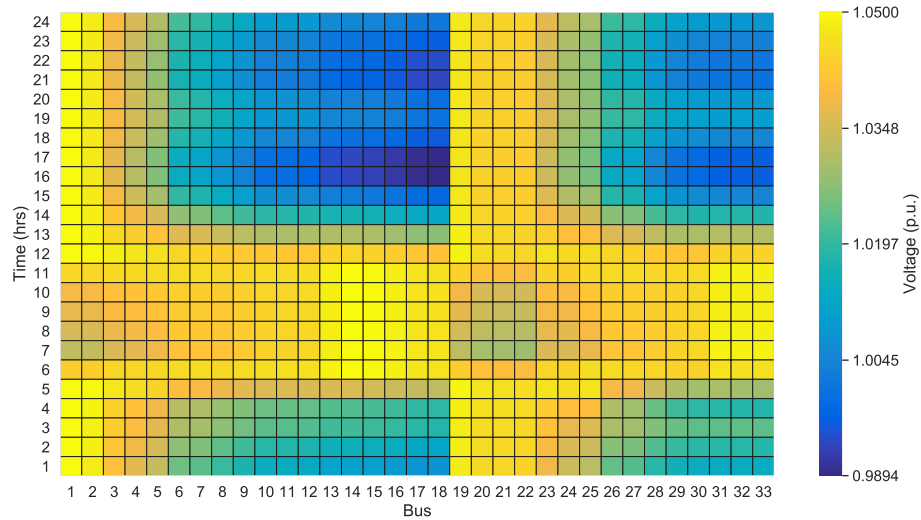
Figure 6.14. System's voltage profiles, Case 4.
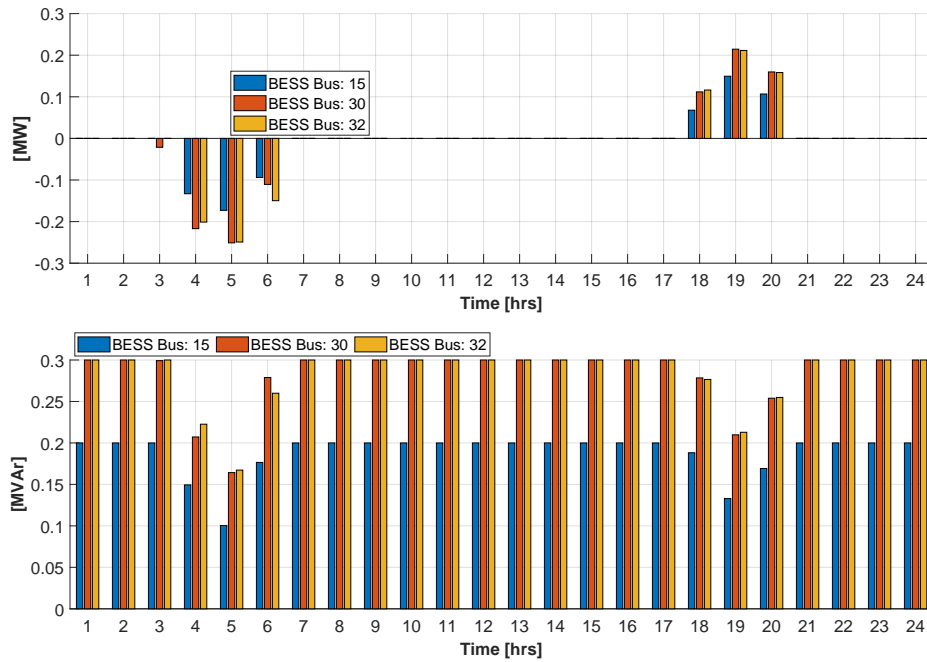
Figure 6.15. BESSs' operation, 24 hrs, Case 4.

Table 6.6 summarizes the results obtained from the cases simulated. When only two wind generators are allocated in the system, there is a reduction in the daily electricity cost of $132.36 and 0.99 MWh in losses. Similarly, when two wind generators and BESSs are considered, the daily saving is equal to $186.47 and
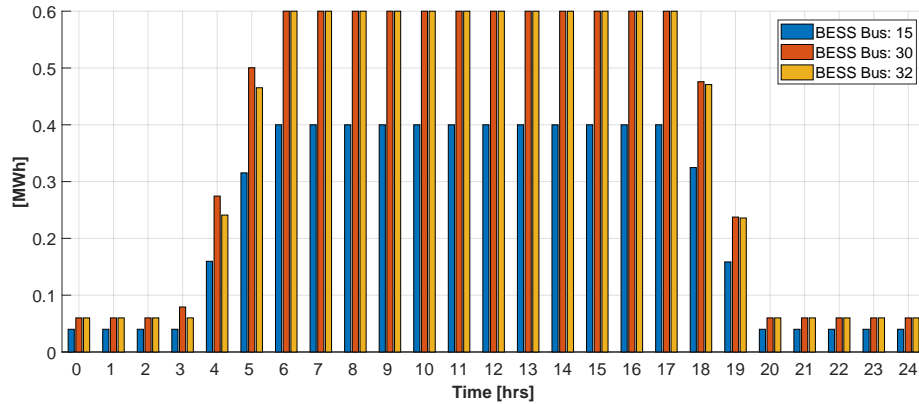
Figure 6.16. Daily energy stored in the BESSs, Case 4.

1.89 MW in losses. Considering the optimal model's parametrization, $N^B = 3$ and $N^{DG} = 5$, produces benefits for the system of \$210.17 and a reduction in energy losses of 2.06 MWh.

Table 6.6. Summary of Results

Case	Electricity cost [\$/day]	BESS investment [\$/day]	Total WTG [MW]	Losses [MWh/day]	Total cost [\$/day]
Case 1	$10,795.78$	0	0	3.28	$10,795.78$
Case 2	$10,663.42$	0	3.168	2.29	$10,663.42$
Case 3	$10,447.51$	161.80	3.366	1.39	$10,609.31$
Case 4	$10,423.80$	161.80	5.346	1.22	$10,585.60$

6.5   Parameters' sensitivity analysis

A series of simulations were performed in order to identify the one-way sensitivity of the results to deviations on the model's parameters. Variation in the range $[-15\%, 15\%]$ in steps of 5% were considered on the daily energy demand, electricity price, and wind speed. For this analysis, the network's benefits were calculated as the difference between the daily system cost with the allocation results of the simulation case 4 and the base-case (system without wind generators and BESSs). The results of these simulations are shown in figure 6.17. When both wind generation and BESS are installed in the network, there are always benefits for the system even with variations in the values of the model's parameters in the range considered. The results show an adequate performance of the solution found.
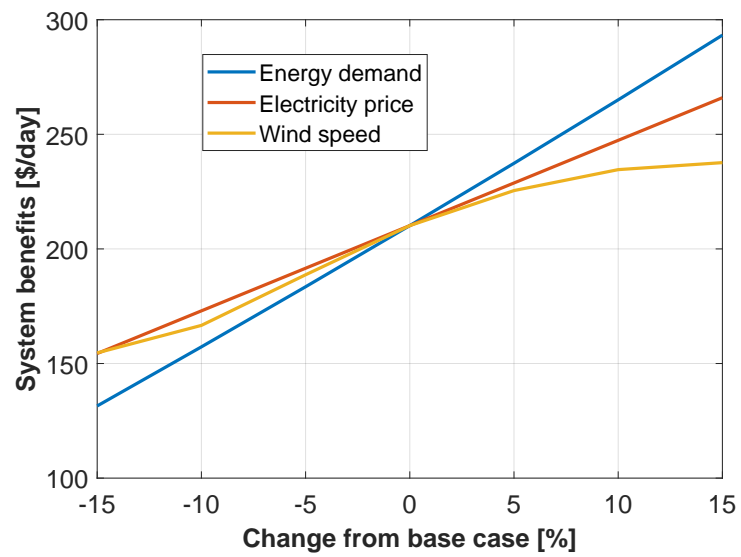
Figure 6.17. Sensitivity analysis for variations on model's parameters.

CHAPTER 7. CONCLUSIONS AND FUTURE WORK

This work has proposed a model for optimal sizing and siting BESSs and distributed generation, in form of wind turbines, in distribution systems to minimize the power generation costs. Furthermore, the methodology provides the storage devices daily optimal operation. To solve the problem, a hybrid approach of genetic algorithm and interior point method in MATPOWER was used. Four simulation cases were carried out in the IEEE 33-bus system to evaluate the system's benefits for optimally incorporating both wind generation and BESSs. The results show that their deployment reduces the system's generation cost through savings on energy demand at peak hours (BESS's energy arbitrage), and power losses. In addition, the daily network operation showed that the BESSs mainly participate in the task of voltage control. The networks voltage profile was notably improved with the wind generation and BESS installation. In terms of connection buses, the BESSs and wind generators were frequently placed at nodes close to the end of the system's branches. The system's benefits were mostly sensible to the distributed generation's penetration levels. In addition, in the system, there were allocated a relatively small number of BESSs due to their high capital cost.

A one-way sensitivity analysis was performed to determine the sensitivity of the system's benefits to small deviations in the energy demand, electricity rates, and wind speed. The results show that there is a linear relationship between the system benefits, and the changes in the energy demand, and electricity prices. The system's benefits were increased in all the cases analyzed with increments in the parameters

considered.

The time needed to solve the proposed model using genetic algorithm can be increased considerably in large-scale networks. The evaluation of the implications of a simplified model that decreases this time could be a potential future research.

In this work, the BESSs only provide support to the DISCOs in the task of energy arbitrage and voltage control. Other evaluations, such as improvements in the network reliability and deferral in network reinforcements, could be evaluated to increase the BESS benefits. Additionally, a deterministic approach was used to evaluate the system's benefits for the incorporation of BESS and wind generation in the distribution network. A stochastic methodology could provide valuable information in the allocation process.

REFERENCES

[1] IRENA, International Renewable Energy Agency.
`https://public.tableau.com/views/IRENARenewableEnergyInsights/`
`Trends?:embed=y&:display_count=no&:toolbar=no`. Accessed: 2019-01-18.

[2] Noshin Omar, Mohamed Daowd, Peter van den Bossche, Omar Hegazy, Jelle
Smekens, Thierry Coosemans, and Joeri van Mierlo. Rechargeable energy
storage systems for plug-in hybrid electric vehiclesassessment of electrical
characteristics. *Energies*, 5(8):2952–2988, 2012.

[3] Musbaudeen O Bamgbopa, Saif Almheiri, and Hong Sun. Prospects of recently
developed membraneless cell designs for redox flow batteries. *Renewable and
Sustainable Energy Reviews*, 70:506–518, 2017.

[4] International Renewable Energy Agency (IRENA). Electricity storage and
renewables: Costs and markets to 2030, 2017. ISBN: 978-92-9260-038-9.

[5] Jason Leadbetter and Lukas G Swan. Selection of battery technology to
support grid-integrated renewable electricity. *Journal of Power Sources*,
216:376–386, 2012.

[6] Southwest Power Pool. Historical load data, 2019.
`https://marketplace.spp.org/pages/hourly-load`, Accessed: 2019-01-15.

[7] NRCS National Water and Climate Center. Soil Climate Analysis Network
(SCAN) Data, 2019.

https://wcc.sc.egov.usda.gov/nwcc/site?sitenum=2001, SCAN Site:
Rogers Farm #1, State: Nebraska, Accessed: 2019-01-15.

[8]   M. E. Baran and F. F. Wu. Network reconfiguration in distribution systems for
      loss reduction and load balancing. *IEEE Transactions on Power Delivery*,
      4(2):1401–1407, April 1989.

[9]   Aventa AG. Wind Turbine Aventa AV-7, 2019.
      https://w3.windfair.net/turbine/91-aventa-av-7, Accessed: 2019-01-15.

[10] JA Pecas Lopes, N Hatziargyriou, J Mutale, P Djapic, and N Jenkins.
      Integrating distributed generation into electric power systems: A review of
      drivers, challenges and opportunities. *Electric power systems research*,
      77(9):1189–1203, 2007.

[11] EIA u.s. energy information administration.
      https://www.eia.gov/todayinenergy/detail.php?id=38053. Accessed:
      2019-02-13.

[12] SN Liew and G Strbac. Maximising penetration of wind generation in existing
      distribution networks. *IEE Proceedings-Generation, Transmission and
      Distribution*, 149(3):256–262, 2002.

[13] Philip P Barker and Robert W De Mello. Determining the impact of
      distributed generation on power systems. i. radial distribution systems. In
      Power Engineering Society Summer Meeting, 2000. IEEE, volume 3, pages
      1645–1656. IEEE, 2000.

[14] Math HJ Bollen and Fainan Hassan. *Integration of distributed generation in the
      power system*, volume 80. John wiley & sons, 2011.

[15] Rajkumar Viral and DK Khatod. Optimal planning of distributed generation systems in distribution system: A review. *Renewable and Sustainable Energy Reviews*, 16(7):5146–5165, 2012.

[16] Roger C Dugan and Thomas E McDermott. Operating conflicts for distributed generation on distribution systems. In *2001 Rural Electric Power Conference. Papers Presented at the 45th Annual Conference (Cat. No. 01CH37214)*, pages A3–1. IEEE, 2001.

[17] Matija Zidar, Pavlos S Georgilakis, Nikos D Hatziargyriou, Tomislav Capuder, and Davor Škrlec. Review of energy storage allocation in power distribution networks: applications, methods and future research. *IET Generation, Transmission & Distribution*, 10(3):645–652, 2016.

[18] Julio Romero Aguero, Erik Takayesu, Damir Novosel, and Ralph Masiello. Modernizing the grid: challenges and opportunities for a sustainable future. *IEEE Power and Energy Magazine*, 15(3):74–83, 2017.

[19] NW Miller, RS Zrebiec, G Hunt, and RW Deimerico. Design and commissioning of a 5 mva, 2.5 mwh battery energy storage system. In *Transmission and Distribution Conference, 1996. Proceedings., 1996 IEEE*, pages 339–345. IEEE, 1996.

[20] Yasser Moustafa Atwa and EF El-Saadany. Optimal allocation of ess in distribution systems with a high penetration of wind energy. *IEEE Transactions on Power Systems*, 25(4):1815–1822, 2010.

[21] Mohammad Rasol Jannesar, Alireza Sedighi, Mehdi Savaghebi, and Josep M Guerrero. Optimal placement, sizing, and daily charge/discharge of battery energy storage in low voltage distribution network with high photovoltaic penetration. *Applied Energy*, 226:957–966, 2018.

[22] Aouss Gabash and Pu Li. Active-reactive optimal power flow in distribution networks with embedded generation and battery storage. *IEEE Transactions on Power Systems*, 27(4):2026–2035, 2012.

[23] Guido Carpinelli, Gianni Celli, Susanna Mocci, Fabio Mottola, Fabrizio Pilo, and Daniela Proto. Optimal integration of distributed energy storage devices in smart grids. *IEEE Transactions on smart grid*, 4(2):985–995, 2013.

[24] Hamidreza Nazaripouya, Yubo Wang, Peter Chu, Hemanshu R Pota, and Rajit Gadh. Optimal sizing and placement of battery energy storage in distribution system based on solar size for voltage regulation. In *Power & Energy Society General Meeting*, pages 1–5, 2015.

[25] Roshni Anna Jacob, Aniruddha Bhattacharya, and Sharmistha Sharma. Planning of battery energy storage system in distribution network considering uncertainty. In *2017 International Conference on Technological Advancements in Power and Energy (TAP Energy)*, pages 1–6. IEEE, 2017.

[26] Nand Kishor Meena, Anil Swarnkar, Nikhil Gupta, and Khaleequr Rehman Niazi. Optimal accommodation and management of high renewable penetration in distribution systems. *IET Journal of Engineering*, 2017.

[27] Amjad Anvari-Moghaddam, Jeremy Dulout, Corinne Alonso, Bruno Jammes, and Josep M Guerrero. Optimal design and operation management of battery-based energy storage systems (bess) in microgrids. In *Advancements in Energy Storage Technologies*. IntechOpen, 2017.

[28] Lazards levelized cost of storage analysis version 3.0. `https://www.lazard.com/media/450338/lazard-levelized-cost-of-storage-version-30.pdf`. Accessed: 2019-02-13.

[29] Lazards levelized cost of storage version 2.0. `https://www.lazard.com/media/438042/lazard-levelized-cost-of-storage-v20.pdf`. Accessed: 2019-02-13.

[30] Enabling modernization of the electric power system, electric energy storage. `https://www.cooperative.com/programs-services/bts/Documents/Reports/Battery-Energy-Storage-Overview-Report-July-2018-Final.pdf`. Quadrennial Technology Review 2015, U.S. DEPARTMENT OF ENERGY; Accessed: 2019-02-13.

[31] KC Divya and Jacob Østergaard. Battery energy storage technology for power systemsan overview. *Electric power systems research*, 79(4):511–520, 2009.

[32] Lithium-based batteries information. `https://batteryuniversity.com/index.php/learn/article/lithium_based_batteries`. Accessed: 2019-02-13.

[33] B. R. Chalamala, T. Soundappan, G. R. Fisher, M. R. Anstey, V. V. Viswanathan, and M. L. Perry. Redox flow batteries: An engineering perspective. *Proceedings of the IEEE*, 102(6):976–999, June 2014.

[34] Chao Zhang, Yi-Li Wei, Peng-Fei Cao, and Meng-Chang Lin. Energy storage system: Current studies on batteries and power condition system. *Renewable and Sustainable Energy Reviews*, 82:3091–3106, 2018.

[35] John K Kaldellis. *Stand-alone and hybrid wind energy systems: technology, energy storage and applications.* Elsevier, 2010.

[36] Ami Joseph and Mohammad Shahidehpour. Battery storage systems in electric power systems. In *2006 IEEE Power Engineering Society General Meeting*, pages 8–pp. IEEE, 2006.

[37] Daniel H Doughty, Paul C Butler, Abbas A Akhil, Nancy H Clark, and John D Boyes. Batteries for large-scale stationary electrical energy storage. *The Electrochemical Society Interface*, 19(3):49–53, 2010.

[38] G Celli and F Pilo. Optimal distributed generation allocation in mv distribution networks. In *pica 2001. Innovative Computing for Power-Electric Energy Meets the Market. 22nd IEEE Power Engineering Society. International Conference on Power Industry Computer Applications (Cat. No. 01CH37195)*, pages 81–86. IEEE, 2001.

[39] Anastasios G Bakirtzis, Pandel N Biskas, Christoforos E Zoumas, and Vasilios Petridis. Optimal power flow by enhanced genetic algorithm. *IEEE Transactions on power Systems*, 17(2):229–236, 2002.

[40] Spyros A Kazarlis, AG Bakirtzis, and Vassilios Petridis. A genetic algorithm solution to the unit commitment problem. *IEEE transactions on power systems*, 11(1):83–92, 1996.

[41] MA Abramson. Genetic algorithm and direct search toolbox users guide. *The MathWorks Inc., Natick, MA*, 2007.

[42] Ray D Zimmerman and Carlos E Murillo-Sanchez. Matpower 7.0b1 user's manual. *Power Systems Engineering Research Center, Cornell University, Ithaca, NY*, 2018.

[43] Southwest Power Pool. Lmp by bus, 2019. `https://marketplace.spp.org/pages/da-lmp-by-bus`, Accessed: 2019-01-15.

[44] Average price of electricity to ultimate customers by end-use sector & state, march 2019 and 2018. `https://www.eia.gov/electricity/monthly/epm_`

`table_grapher.php?t=epmt_5_6_a`. U.S. Energy Information Administration - EIA, Accessed: 2019-05-25.

[45] Sébastien Le Digabel. Algorithm 909: Nomad: Nonlinear optimization with the mads algorithm. *ACM Transactions on Mathematical Software (TOMS)*, 37(4):44, 2011.

[46] Battery energy storage technology assessment, platte river power authority. `https://www.prpa.org/wp-content/uploads/2017/10/` `HDR-Battery-Energy-Storage-Assessment.pdf`. Accessed: 2019-05-15.

[47] Hrvoje Pandžić, Yishen Wang, Ting Qiu, Yury Dvorkin, and Daniel S Kirschen. Near-optimal method for siting and sizing of distributed storage in a transmission network. *IEEE Transactions on Power Systems*, 30(5):2288–2300, 2014.

APPENDIX A. NOMENCLATURE

A.1   Functions

z Objective function

P_t^W Base wind generator active power production at time t

A.2   Indices and sets

i, j Buses index

t Period in hours

Ω^{N_f} Set of BESS and DG's feasible connection buses

Ω^N Set of networks buses

Ω^T Set of period of analysis t

A.3   Wind turbine Parameters

$v_{c_{in}}$ Wind turbine designing cut-in wind speed

$v_{c_{out}}$ Wind turbine designing cut-out wind speed

v_r Wind turbine wind speed rating

$P^{TB_{nom}}$ Wind turbine power rating

A.4 Battery system Parameters

C^B BESS' capital cost per day (Base unit) $\$/day$

DoD^{B_u} Battery depth of discharge (Base unit) [%]

$\overline{S}^{B_u}$ Nominal capacity of apparent power [kVA](BESS Base unit)

$\overline{E}^{B_u}$ Nominal capacity of energy storage [kWh] (BESS Base unit)

η_{ch}/η_{dis} Charging/discharging efficiency (BESS Base unit)

A.5 Distribution system network parameters

$Y_{i,j}$ Magnitude of the element of the admittance matrix in the entry (i,j)

$\theta_{i,j}$ Angle of the element of the admittance matrix in the entry (i,j)

$\overline{S}_{i,j}$ Power rating of transmission line between bus i and bus j

$\underline{V}$ Minimum network's voltage limit

$\overline{V}$ Maximum network's voltage limit

$P^D_{i,t}$ Active power demand at but i at time t

$Q^D_{i,t}$ Reactive power demand at but i at time t

A.6 Model parameters

$\overline{P}^{Sub}$ System's main substation power rating

N^{DG} Maximum number of wind generators to install in the system

N^B Maximum number of BESSs to install in the system

C^E_t Electricity cost at period t

$v_{wind}(t)$ — Wind speed at period t

M — A large positive number

A.7 Model variables

$\overline{E}_i^B$ — $BESS$ at node i's nominal energy storage capacity [kWh]

$\underline{E}_i^B$ — $BESS$ at node i's minimum energy stored limits [kWh]

$E_{i,t}^B$ — $BESS$ at node i's energy stored at period t [kWh]

$\overline{S}_i^B$ — BESS at node i's nominal apparent power capacity [kVA]

$P_{i,j,t}$ — Real power flow at transmission line between node i and node j

$Q_{i,t}$ — Reactive power flow at transmission line between node i and node j

$P_{i,t}$ — Sum of active power flow through the transmission lines connected to node i

$Q_{i,t}$ — Sum of reactive power flow through the transmission lines connected to node i

$Q_{i,t}^{DG}$ — Reactive power injected at node i at time t by a wind generator

A.8 GA parameters

$\chi^B{}_s$ — BESS s location

Φ_s^B — BESS s size

χ^{DG} — Wind generator s connection node

Φ_s^{DG} — Wind generator s size

ω Penalty factor of the inequality constraint for the maximum wind generation installed capacity

A.9   Model decision variables

φ_i^B Integer number, indicates the number of batteries modules in the BESS to install at node i

x_i^B Binary variable,$\{0,1\}$, indicates the installation of a BESS in node i when $x_i^B = 1$

φ_i^{DG} Integer number, indicates the number of wind turbines in the wind generator installed at node i

x_i^{DG} Binary variable,$\{0,1\}$, indicates the installation of a wind generator at node i when $x_i^{DG} = 1$

$v_{i,t}$ Node i's voltage magnitude at time t

$\delta_{i,t}$ Node i's voltage angle at time t

$p_{i,t}^{Grid}$ Grid's active power injection at node $i = 1$ at time t

$q_{i,t}^{Grid}$ Grid's reactive power injection at node $i = 1$ at time t

$p_{i,t}^{ch,B}$ Active charging power at period t of the BESS installed at node i

$p_{i,t}^{dis,B}$ Active discharging power at period t of the BESS installed at node i

$q_{i,t}^B$ Reactive power output/input at period t of the BESS installed at node i

APPENDIX B. ACRONYMS

$BESS$	Battery Energy Storage System
$DISCO$	Distribution System Company
DG	Distributed Generation
AC-MPOPF	AC Multi-period Optimal Power Flow
$AC - OPF$	AC Optimal Power Flow
PCS	Power Conversion System
LMP	Local Marginal Price
$OLTC$	On-Load Tap Changer Transformer
ESS	Energy Storage System
$DESS$	Distributed Energy Storage System
SG	Smart Grid
WTG	Wind Turbine Generator
GA	Genetic algorithm

APPENDIX C. SIMULATION PARAMETERS

Table C.1. 33-Bus test system - Network data [8].
$S_{base} = 10$ MVA, $V_{base} = 12.66\ kV$, $\overline{V} = 1.05\ p.u., \underline{V} = 0.95\ p.u., \overline{S}_{i,j} = 6$ MVA

Line No.	From Bus	To Bus	R (ohm)	X (ohm)	P (kW)	Q (kvar)
1	1	2	0.0092	0.0048	100.00	60.00
2	2	3	0.0493	0.0251	90.00	40.00
3	3	4	0.0366	0.0186	120.00	80.00
4	4	5	0.0381	0.0194	60.00	30.00
5	5	6	0.0819	0.0707	60.00	20.00
6	6	7	0.0187	0.0619	200.00	100.00
7	7	8	0.1711	0.1235	200.00	100.00
8	8	9	0.1030	0.0740	60.00	20.00
9	9	10	0.1040	0.0740	60.00	20.00
10	10	11	0.0200	0.0065	45.00	30.00
11	11	12	0.0374	0.0124	60.00	35.00
12	12	13	0.1468	0.1155	60.00	35.00
13	13	14	0.0542	0.0713	120.00	80.00
14	14	15	0.0591	0.0526	60.00	10.00
15	15	16	0.0746	0.0545	60.00	20.00
16	16	17	0.1289	0.1721	60.00	20.00
17	17	18	0.0732	0.0574	90.00	40.00
18	2	19	0.0164	0.0156	90.00	40.00
19	19	20	0.1504	0.1355	90.00	40.00
20	20	21	0.0410	0.0478	90.00	40.00
21	21	22	0.0709	0.0937	90.00	40.00
22	3	23	0.0451	0.0308	90.00	50.00
23	23	24	0.0898	0.0709	420.00	200.00
24	24	25	0.0896	0.0701	420.00	200.00
25	6	26	0.0203	0.0103	60.00	25.00
26	26	27	0.0284	0.0145	60.00	25.00
27	27	28	0.1059	0.0934	60.00	20.00
28	28	29	0.0804	0.0701	120.00	70.00
29	29	30	0.0507	0.0259	200.00	600.00
30	30	31	0.0974	0.0963	150.00	70.00
31	31	32	0.0310	0.0362	210.00	100.00
32	32	33	0.0341	0.0530	60.00	40.00

Equation C.1 is used to find the BESS base unit's daily capital cost
considering its energy capacity. Similarly, the BESS base unit's daily capital cost

Table C.2. BESS base unit parameters.

Parameter	Unit	Value
Project Life (n)	years	20 [47]
Apparent power rating $(\overline{S}^{B_u})$	kVA	50.0
Energy storage capacity $(\overline{E}^{B_u})$	kWh	100.0
Charging efficiency of storage	%	90.0 [47]
Discharging efficiency of storage	%	90.0 [47]
Depth of discharge	%	10.0
Capital cost (C_e)	$/kWh	340.0 [46]
Capital cost (C_p)	$/kVA	240.0 [46]
Interest rate (r)	%	5.0 [47]
Capital cost per day (C^B)	$/day	10.11

based on its power rating is calculated through equation C.2.

$$In_E = \overline{E}^{B_u} \cdot C_e \cdot \frac{r(1+r)^n}{(1+r)^n - 1} \cdot \frac{1}{365} \tag{C.1}$$

$$In_P = \overline{S}^{B_u} \cdot C_p \cdot \frac{r(1+r)^n}{(1+r)^n - 1} \cdot \frac{1}{365} \tag{C.2}$$

The battery base unit's cost per day C^B is then defined by equation C.3.

$$C^B = In_E + In_P \tag{C.3}$$

Table C.3. Wind turbine base unit parameters [9].

Parameter	Value
Rated Power	6.0 (kW)
Rated speed	4.5 (m/s)
Cut-in speed	2.0 (m/s)
Cut-out speed	14.0 (m/s)